**UNIVERSIDADE DE LISBOA**

**FACULDADE DE CIÊNCIAS**

Departamento de Biologia Vegetal

# The role of Notch signaling in thymic and parathyroid glands organogenesis

**Joana Clara Silva**

Dissertação

**MESTRADO EM BIOLOGIA MOLECULAR E GENÉTICA**

**2013**

**UNIVERSIDADE DE LISBOA**

**FACULDADE DE CIÊNCIAS**

Departamento de Biologia Vegetal

# The role of Notch signaling in thymic and parathyroid glands organogenesis

**Joana Clara Silva**

**Dissertação orientada por:**

Pofessora Doutora Hélia Cristina de Oliveira Neves (FMUL)

Professora Doutora Rita Maria Pulido Garcia Zilhão (FCUL)

**MESTRADO EM BIOLOGIA MOLECULAR E GENÉTICA**

**2013**

**AGRADECIMENTOS**

Em primeiro lugar, agradeço à professora Hélia, pela oportunidade que me deu de fazer parte do seu grupo. Pela sua orientação, dedicação, preocupação e por toda a confiança que depositou em mim e no meu trabalho, desde o primeiro dia. Por nunca ter levado a mal alguma irreverência que sei ser-me muito própria mas, acima de tudo, agradeço a sua enormíssima compreensão, e por ter sempre percebido o que eu precisava quando me faltavam palavras para fazer pedidos.

Em segundo lugar, agradeço à professora Rita, por me ter dado a conhecer este grupo extraordinário. Por todos os seus conselhos e palavras, e pelo entusiasmo diário com que partilha os seus conhecimentos. Por ser um exemplo a seguir.

A toda a Unidade de Biologia da Hematopoiese do Instituto de Histologia e Biologia do Desenvolvimento da FMUL. Em particular, à Sofia, por ter feito isto comigo. Pela sua companhia e boa disposição, e por ter tornado mais fácil a minha integração não-solitária. Ao Vítor, que considero uma peça fundamental, por toda a ajuda na integração inicial e disponibilidade total. Ao Pedro, pela sua companhia diária, e à Margarida e à Carlota, que tornavam o nosso espaço mais preenchido e, consequentemente, mais alegre. À professora Isabel pela sua constante simpatia e preocupação.

De entre todos os que durante este ano demonstraram o seu interesse e preocupação com o meu trabalho tenho, inevitavelmente, alguns agradecimentos especiais a fazer.

À ELITE, pelas recorrentes combinações de sextas à noite e por me terem arrastado com eles para uns dias de férias. Acima de tudo, por valorizarem os anos de amizade e pelo esforço que cada um faz para a manter.

Aos Fofinhos, onde incluo a Filipa, pelas inúmeras tardes de esforço conjunto. Pela boa companhia e sentido de humor, que tornaram todos esses dias intermináveis em momentos de diversão e descontração. Por termos feito um percurso diferente mas sempre lado-a-lado, ao mesmo nível, o que constitui para mim um motivo de enorme orgulho.

À Lili, Teresa, Andreia e Luísa pelos anos de amizade. Por me terem sempre feito sentir como sendo parte do grupo, mesmo sem eu saber como lá fui parar. Pelos mesmos motivos, um obrigada especial à Marta Reis, por me deixar raptá-la quando preciso de apanhar ar. Por me ouvir sem questionar, e por todos os conselhos e ajudas imprescindíveis (podes começar a tratar do teleponto). À Carolina e à Bia, pela amizade e companhia durante todo o último ano, pelas conversas, pelos conselhos e por me ouvirem.

A toda a equipa de Voleibol da FCUL, sem excepção. Pela quantidade e qualidade de momentos passados nos últimos 5 anos, e por contribuírem semanalmente para a

manutenção da minha sanidade mental. Acredito que me ajudaram a crescer enquanto pessoa e que sem isso não teria sido capaz de estar hoje onde estou.

À Leonor e à Renata, por serem a prova de que a distância nem sempre altera a forma como vemos as pessoas. Por estarem sempre presentes quando é preciso e pela amizade, apoio e ajuda fundamentais ao longo dos últimos anos. Pelas mesmas razões, agradeço ao Francisco, que mesmo longe disponibilizou prontamente o seu tempo para me ajudar a resolver questões relacionadas com este trabalho. É sem surpresa mas com orgulho que olho para o seu percurso e o vejo como um exemplo.

À Rita, que por ser tão parecida comigo em tanta coisa, me compreende. Pela companhia durante o primeiro ano de mestrado, que teria sido (ainda mais) desesperante se não tivesse havido a partilha de espírito crítico que ainda hoje mantemos. Pelo seu sentido de humor e pela sua excelência, e por muitas vezes acreditar mais em mim do que eu própria, obrigando-me a ser sempre melhor. Acima de tudo, pela sua preocupação e dedicação em manter-se em contacto apesar da distância, e pela confiança que tem nas minhas capacidades.

Ao Diogo, pela amizade de anos. Pelo apoio incondicional em todas as etapas da minha vida e por fazer parte de todas elas. Pela sua genialidade e criatividade que todos os dias me fascinam e por corresponder sempre às expectativas. É com orgulho que vejo a pessoa em que se tornou, especialmente por todas as dificuldades que encontrou e continua a encontrar no caminho. Por fazer dos meus sonhos os sonhos dele e fazer de tudo para os realizar.

Ao Pedro, por tudo o que me ensinou na vida, muitas vezes apenas pelo seu discurso introspectivo. Pela partilha de todas as suas fantásticas experiências e por ironicamente ter sido a minha companhia nos momentos mais difíceis.

À minha família, pela confiança ilimitada nas minhas capacidades e pelo suporte financeiro e moral de 22 anos de vida. Em especial, ao meu irmão, pela sua preocupação e por todas as suas tentativas de perceber o que eu faço ou estudo.

Por último, mas em destaque, um especial e inevitável agradecimento à Marta, a quem me vão faltar palavras para agradecer tudo o que devo. Por ser garantidamente uma das pessoas mais extraordinárias e completas que conheço. O seu apoio, preocupação e palavras foram de uma importância incalculável durantes os vários momentos menos bons que passei este ano. Pela capacidade infinita que tem de gerar boa disposição à sua volta. Por partilhar todo o seu conhecimento de uma forma tão simples. Por fazer sempre tudo bem. Sem ela este trabalho não teria sido possível.

**RESUMO**

O timo é um órgão essencial do sistema imunitário, cuja função é gerar linfócitos T auto-restritos e auto-tolerantes que entram em circulação, onde actuam como parte da resposta imune adaptativa. Histologicamente, o timo encontra-se dividido em duas regiões - o córtex e a medula - que se caracterizam pela presença de diferentes Células Epiteliais Tímicas (CETs): corticais (cCETs) ou medulares (mCETs), respectivamente. A função do timo na diferenciação e maturação de linfócitos T é indissociável da função especializada destes dois tipos celulares, assim como da própria arquitectura do órgão.

Anatomicamente próximas do timo mas com uma função absolutamente distinta, as glândulas paratiróides são responsáveis pela regulação da homeostase do cálcio extracelular. Quando os seus receptores detectam alterações nos níveis de cálcio no sangue, as células epiteliais sintetizam e secretam a hormona paratiróide que actua em diferentes alvos de forma a permitir o restabelecimento homeostático.

Apesar das diferenças funcionais e estruturais, o desenvolvimento destes dois órgãos está intimamente ligado, uma vez que os seus epitélios partilham a mesma origem embrionária – a endoderme da 3ª e 4ª bolsas faríngicas (3/4 BF, em galinha). Os rudimentos do timo e das glândulas paratiróides encontram-se assim identificados pela expressão regionalizada dos marcadores moleculares *Foxn1* (Forkhead box N1) e *Gcm2* (Glial cells missing-2) na endoderme da 3/4 BF, respectivamente.

A origem endodérmica das CETs, assim como a importância das interacções epitélio-mesenquimais na sua especificação, foram primariamente evidenciadas por Le Douarin e Jotereau, utilizando o modelo de quimeras galinha-codorniz. A capacidade de distintos mesênquimas ectópicos suportarem (mesênquima permissivo da somatopleura) ou não (mesênquima não permissivo do botão do membro) o desenvolvimento da endoderme da 3/4 BF na formação de um timo funcional, revela a importância destas interacções na especificação das CETs. Para além disso, um estudo recente identificou dois factores de transcrição, Bmp4 e Fgf10, cuja expressão sequencial na endoderme e no mesênquima é fundamental para especificação da endoderme da 3/4 BF nos epitélios do timo e das glândulas paratiróides.

A sinalização Notch é uma via de sinalização celular que regula aspectos como a proliferação, destino, sobrevivência e diferenciação celular no desenvolvimento embrionário e no adulto. A sua importância no normal funcionamento do sistema imunitário, nomeadamente na hematopoiese e linfopoiese, é bem conhecida. De facto, foi demonstrado que a geração das primeiras células estaminais hematopoiéticas assim como a especificação dos progenitores hematopoiéticos nas diferentes linhagens linfoides são

acontecimentos dependentes da sinalização Notch. Adicionalmente, a expressão de genes ligados à sinalização Notch em diferentes territórios do timo adulto e a observação do seu envolvimento na diferenciação de linfócitos mas também na diferenciação dos dois tipos de CETs, sugere o envolvimento desta sinalização na organogénese tardia do timo. Existem, no entanto, poucas evidências da sua função nos estadios iniciais da organogénese do timo. Recentemente, o nosso grupo de investigação observou a expressão de genes envolvidos na sinalização Notch, nomeadamente ligandos, receptores e genes-alvo, nos territórios presuntivos do timo e das glândulas paratiróides. Adicionando a conhecida importância desta sinalização no desenvolvimento e função do timo adulto, estas evidências apontam para um papel relevante da sinalização Notch também na fase inicial do desenvolvimento destes dois órgãos.

Neste projecto pretendeu-se estudar o papel da sinalização Notch durante os estadios iniciais de desenvolvimento do timo e das glândulas paratiróides, utilizando para isso os modelos de galinha e codorniz. De forma a manipular a sinalização Notch nos territórios presuntivos do timo e das paratiróides foram desenvolvidos dois sistemas organotípicos *in vitro*: explantes da região faríngica de embriões de codorniz com 3 dias de desenvolvimento; e associações heteroespecíficas da endoderme da 3/4 BF com mesênquima ectópico permissivo da somatopleura (previamente desenvolvido no laboratório, Neves et al, 2012).

No primeiro sistema, a estrutura tridimensional da região faríngica é mantida intacta, preservando o contacto da endoderme da 3/4 BF com os tecidos envolventes (mesênquima e ectoderme). Para testar o efeito da inibição farmacológica da sinalização Notch nos estadios iniciais de desenvolvimento do timo e das glândulas paratiróides, os explantes da região faríngica foram mantidos em contacto com dois tipos de inibidores da $\gamma$-secretase (cuja função é necessária para a normal sinalização): DAPT e LY411575. A capacidade de inibição da sinalização Notch e o seu efeito na formação do timo e das glândulas paratiróides foram avaliados pela expressão de *Hes5.1*, *Foxn1* e *Gcm2*, respectivamente, por PCR quantitativo em tempo real (qRT-PCR). Os nossos dados indicam que a inibição da sinalização Notch tende a diminuir a expressão de *Foxn1* e *Gcm2*, sugerindo que o desenvolvimento dos dois órgãos se encontra comprometido na ausência de sinais Notch.

O segundo sistema consiste na associação heteroespecífica de endoderme da 3/4 BF de codorniz com mesênquima permissivo da somatopleura de galinha. Esta abordagem permite a manipulação da sinalização Notch especificamente nos territórios presuntivos do timo e das glândulas paratiróides e sua posterior associação a um mesênquima ectópico, necessário para o seu desenvolvimento. Para validar o sistema anterior de inibição da sinalização Notch nos explantes da região faríngica, esta associação de tecidos foi igualmente sujeita a inibição farmacológica da sinalização Notch, como descrito

anteriormente. Uma vez mais, os resultados indicam que a ausência de sinais Notch compromete a normal organogénese do timo e das glândulas paratiróides.

Para modificar a sinalização Notch de forma estável e a nível celular na endoderme da 3/4 BF, foi usado um sistema de vectores que combina a "transferência génica mediada por *Tol2*" e a "expressão condicional dependente de tetraciclina". Assim, a endoderme da 3/4 BF foi geneticamente modificada de forma a promover um ganho ou perda de função da sinalização Notch. Para ganho de função, a endoderme da 3/4 BF foi electroporada com um conjunto de vectores que induzem a expressão da forma intracelular do receptor Notch1 (ICN1), que se sabe activar a sinalização Notch de forma constitutiva e independente da ligação a um ligando. Para perda de função, o mesmo sistema foi utilizado, mas forçando a expressão de uma forma dominante-negativa do co-activador Mastermind-like1 (DNMAML1). Neste contexto, foi construído neste trabalho um novo vector para perda de função com o objectivo de aumentar a estabilidade da proteína DNMAML1 (que tem apenas 205 pares de bases) e de a direcionar para o núcleo por adição de uma sequência com um sinal de localização nuclear, aumentando a sua eficiência. Estas abordagens permitiram testar o efeito da modulação do sinal Notch durante as interacções epitélio-mesenquimais necessárias para a formação dos dois órgãos em estudo, pela avaliação dos níveis de expressão de *Foxn1* e *Gcm2*. Inesperadamente, os resultados de perda e ganho de função mostram uma tendência de fenótipo semelhante, com a descida da expressão de *Foxn1* e o aumento da expressão de *Gcm2*, em ambos os casos. Estes dados demonstram que a perda de função da sinalização Notch especificamente no domínio presuntivo do timo e das glândulas paratiróides tem um efeito diferente do obtido quando toda a região faríngica é sujeita a inibição. Ficam no entanto por aferir as condições deste sistema para ganho de função da sinalização Notch.

**Palavras-chave:** sinalização Notch; organogénese; timo; glândulas paratiróides; qRT-PCR; sistema organotípico *in vivo*;

**ABSTRACT**

The thymus is the organ responsible for the differentiation and maturation of Lymphoid Progenitor Cells into T lymphocytes, while the parathyroid glands have a key role in the regulation of the extracellular calcium homeostasis by the production of the parathyroid hormone. Despite their functional differences, the epithelia of these organs derive from the endoderm of the 3$^{rd}$ and 4$^{th}$ pharyngeal pouches (3/4 PP), in avian.

Notch signaling has been implicated in several aspects of organogenesis, inclusively having a function during the late stages of thymus development. A recent observation from our group showed Notch-related genes expression in the 3/4 PP endoderm and surrounding mesenchyme suggesting a role for Notch signaling in the thymic and parathyroid glands early-organogenesis.

In this study, we investigated Notch signaling effects in avian thymus and parathyroid glands early-organogenesis. For that, we modulated Notch signals in their prospective territories, prior to organ formation. In a first assay, explants of the pharyngeal region of E3 quail embryos were grown in the presence of Notch signaling inhibitors (DAPT or LY411575). After 48h of culture, the expression *Hes5.1* (Notch-target gene), *Foxn1* (marker for thymus epithelium) and *Gcm2* (marker for parathyroid glands epithelium) was evaluated by qRT-PCR. The results showed that the pharmacological inhibition of Notch signaling promoted a decrease of *Foxn1* and *Gcm2* expression, suggesting that blocking Notch signaling impairs normal early stages of thymus and parathyroid glands development. Moreover, studies were performed to modulate Notch signaling (gain- and loss-of-function) specifically in the prospective territories of the thymus and parathyroid glands (3/4 PP). In this context, I developed a new loss-of-function construct (pT2K-NLS-Cherry-DNMAML1-eGFP). Both in gain- or loss-of-function experiments, the expression of *Foxn1* was down-regulated and the expression of *Gcm2* was up-regulated. This conflicting data will be subject to further study.

**Keywords:** Notch signaling; early-organogenesis; thymus; parathyroid glands; qRT-PCR;

## TABLE OF CONTENTS

## LIST OF FIGURES

## LIST OF TABLES

**LIST OF ABBREVIATIONS**

| | |
|---|---|
| **aa** | amino acid |
| **bp** | base pairs |
| **cDNA** | complementary Deoxyribonucleic Acid |
| **DAPT** | N-[N-(3,5-Difluorophenacetyl-L-alanyl)]-S-phenylglycine t-Butyl Ester |
| **DMSO** | Dimethyl sulfoxide |
| **DN** | Dominant Negative |
| **DNA** | Deoxyribonucleic Acid |
| **dNTP** | Deoxynucleotide triphosphate |
| **Dox** | Doxycycline |
| **DTT** | Dithiothreitol |
| **E** | Embryonic day of development |
| **F** | Farad |
| **FBS** | Fetal Bovine Serum |
| **GAPDH** | Glyceraldehyde-3-Phosphate Dehydrogenase |
| **GFP** | Green Fluorescence Protein |
| **h, min, sec** | hour, minute, second |
| **ICN** | Intracellular domain of Notch |
| **LB** | Lysogeny Broth |
| **LPC** | Lymphoid Progenitor Cell |
| **NC** | Neural Crest |
| **NLS** | Nuclear Localisation Signal |
| **PA** | Pharyngeal Arch |
| **PBS** | Phosphate Buffered Saline |
| **Pen/Strep** | Penicillin/Streptomycin |
| **PP** | Pharyngeal Pouch |
| **PTH** | Parathyroid Hormone |
| **qRT-PCR** | Quantitative Real-Time Polymerase Chain Reaction |
| **RNA** | Ribonucleic Acid |
| **rpm** | Revolutions per minute |
| **RT** | Room Temperature |
| **StDev** | Standard-deviation |
| **TEC** | Thymic Epithelial Cell |
| **UV** | Ultraviolet |
| **V** | Volts |
| **WM** | Whole-mount |

# 1. INTRODUCTION

## 1.1. The morphology and function of the thymus

The thymus is a primary lymphoid organ responsible for the differentiation of Lymphoid Progenitor Cells (LPCs) into T lymphocytes, a key cellular component of the adaptive immune response. T cell development begins when the LPCs enter the thymus and it is characterized by the thymocyte (developing T lymphocyte) progression through several phenotypically distinct stages (Blackburn and Manley, 2004).

Surrounded by a mesenchymal capsule, the thymus is divided into two main histologically distinct regions - the cortex and the medulla, characterized by the presence of different subsets of stromal cells, the cortical (c) and medullary (m) Thymic Epithelial Cells (TECs). Thymocytes are more than 95% of the cells in the thymus, and their differentiation is intimately dependent on their interaction with cTECs and mTECs as well as mesenchymal cells, endothelial cells, dendritic cells and macrophages, in which complex signals drive the commitment and differentiation into the T cell lineage (Gordon and Manley, 2011). After entering the thymus at the cortico-medullary junction, the LPCs travel throughout the thymic cortex, where cTECs drive their commitment, proliferation and rearrangement and expression of T cell receptors (TCRs). Thymocytes with the ability to recognize self-antigens expressed by cTECs undergo positive selection, receiving survival and maturation signals, and traveling into the medulla. Once in the medulla, thymocytes that react to tissue-restricted self-antigens expressed by mTECs are negatively selected, giving rise to only self-restricted and self-tolerant mature T lymphocytes that enter the circulation (Palmer, 2003; Ladi et al., 2006; Ge and Zhao, 2013).

In mammals and birds, the thymus starts to involute early in the development (6 weeks after birth in mice, 1 year in human and $3^{rd}/4^{th}$ month after birth in chicken), affecting both T cell production and thymic microenvironment maintenance resulting in a decrease in functional thymic volume (Dorshkind et al., 2009; Shanley et al., 2009; Tarek et al., 2012). It is therefore crucial the correct patterning and organization of thymic stromal components for an efficient thymic function. Defects in thymus structure and function normally generate problems such as immunodeficiency and autoimmunity, urging the importance of unrevealing the developmental processes underlying thymic organogenesis (Nowell et al., 2007).

## 1.2. The morphology and function of the parathyroid glands

The parathyroid glands play a key role in the regulation of extracellular calcium homeostasis, which is important to many physiological processes such as muscle contraction, blood coagulation and synaptic activity. Through calcium-sensing receptor (CasR), these glands are able to detect changes in the levels of calcium in the blood and

produce the parathyroid hormone (PTH). For instance, when low calcium levels are detected in blood, the parathyroid glands produce and secrete PTH that directly targets receptors on osteoblasts to regulate bone resorption. In the kidney, PTH targets distal tubule epithelial cells, increasing renal calcium reabsorption, allowing the increase of calcium in blood (Okabe and Graham, 2004; Liu et al., 2007).

Histologically, parathyroid glands have a thin capsule of collagen I and III (reticular fibers) and few elastic fibers that surround a parenchyma, where the epithelial cells (chief cells) are responsible for the PTH synthesis (Gilmour, 1939). Mutations in genes that act during parathyroid development impair PTH production, causing a disease called hypoparathyroidism (Liu et al., 2007). To better understand the development of this and other parathyroid disorders it is important to comprehend parathyroid glands organogenesis.

Despite their structural and functional differences, the development of the thymus and parathyroid glands is intimately linked – the epithelium of both organs derives from the endoderm of the pharyngeal pouches (PP) (Gordon and Manley, 2011). However, the precise PP embryological origin, the number of organs formed and the final anatomical positions of these organs differ according to the species (Rodewald, 2008). For instance, in mammals, the thymus is a bilobed organ centrally located on the thoracic cavity, above the heart and behind the sternum (Gordon and Manley, 2011), whereas pairs of parathyroid glands are located in the dorsal region of the thyroid gland. In birds, the thymus is subdivided in seven lobes that are bilaterally located along the neck, near the jugular vein. The pair of parathyroid glands is located at the bottom of each thymic cord, under the thyroid glands (Neves et al., 2012).

### 1.3. The organogenesis of the thymus and parathyroid glands

The epithelia of the thymus and parathyroid glands share the same embryological origin – the endoderm of the PP. The pharyngeal apparatus arises from a series of bulges on the lateral surface of the head of the embryo, the pharyngeal arches (PA), covered on the outside by the ectoderm, and on the inside by the endoderm, having a core of neural crest (NC)-derived mesenchymal cells (**Figure 1-1**). Five pairs of PA emerge between Theiler's stages 13 (St13) and St16 in the mouse and Hamburger and Hamilton stages 14 (HH14) and HH19 in the chick. The endoderm of the pharyngeal tube evaginates between the adjacent arches, forming an out-pocketing – the PP, while the external overlying ectoderm depresses forming a pharyngeal cleft (Grevellec and Tucker, 2010; Graham and Richardson, 2012).

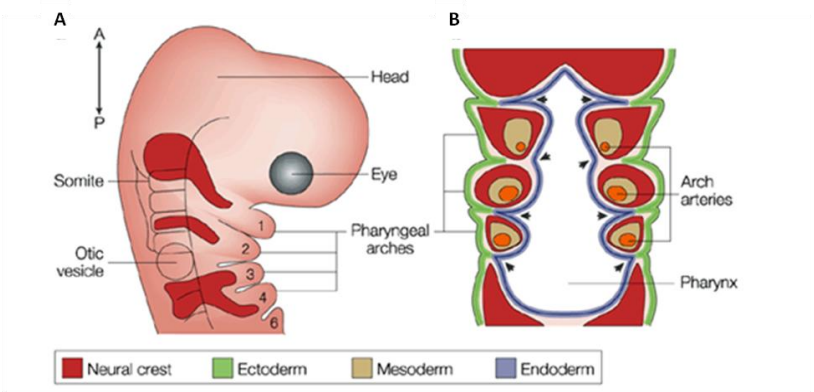


**Figure 1-1 The pharyngeal apparatus.** A side view of the PA pairs of a HH16 chick embryo **(A)**. A longitudinal section through the PA highlighting the contribution of the three embryonic tissue layers (ectoderm, mesoderm and endoderm) **(B)**. Arrows indicate the PP (1st to the 4th PP); A, Anterior; P, Posterior. Adapted from Lindsay, 2001.

In 1975, using the chick-quail chimeras system it was shown that TECs derive from the PP endoderm (Douarin and Jotereau, 1975). Later on it was shown that, in mice, the rudiments of parathyroid glands and thymus emerge from the 3rd PP (3PP) endoderm (Gordon et al., 2001), while in human emerge from the 3rd and 4th PP (3/4 PP) and the 3PP, respectively (Farley et al., 2013). In birds, such as chicken and quail, the rudiments of the two organs derive from the endoderm of the 3/4 PP (Douarin and Jotereau, 1975; Neves et al., 2012).

In mice, the 3PP appears at Embryonic day of development 9.5 (E9.5) and is patterned into organ-specific domains by the regionalized expression of molecular markers. More precisely, the parathyroid domain identity is specifically determined by the expression of *Gcm2* (the mouse homolog of the *Drosophila* transcription factor Glial Cells Missing), which is first detected at E9.5 in an anterior/dorsal region. *Gcm2* deletion results in the absence of parathyroid glands showing that *Gcm2* is essential for the survival and differentiation of these glands (Günther et al., 2000). Conversely, the thymus domain identity is specified by the expression of the transcription factor forkhead box N1 (*Foxn1*) at E11.25 in a posterior/ventral domain (Patel et al., 2006; Gordon et al., 2001; Gordon and Manley, 2011). Mice deficient for *Foxn1* (nude mouse) have a hairless phenotype and are athymic. Furthermore, in nude mouse the LPCs fail to enter the thymic primordium (Itoi et al., 2001) and TECs fail to proliferate and differentiate (Blackburn et al., 1996).

In chicken, the rudiments of the thymus and parathyroid glands are also identified by the distinct domains of *Gcm2* and *Foxn1* expression in the 3/4 PP, respectively. *Gcm2* is detected by RT-PCR from E3 onwards (E2.5 in quail) in a medial/anterior domain of the pouches (**Figure 1-2 A and B**), while *Foxn1* is detected at E4 (E3.5 in quail) and is confined to a dorsal region (**Figure 1-2 C and D**). These divergent expression domains of the organ-specific markers might explain the different final anatomical positions of the adult thymus in mammals and birds (Neves et al., 2012).

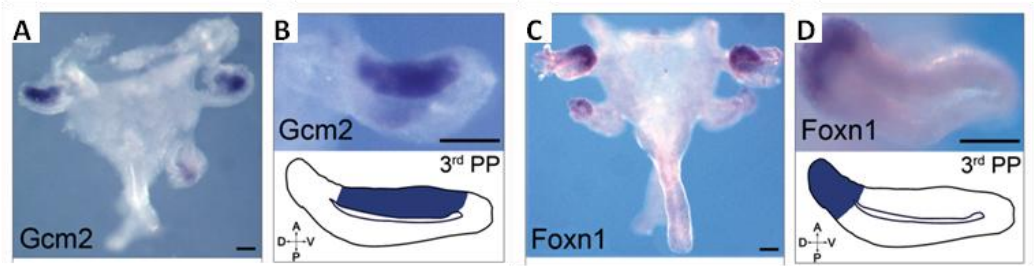


**Figure 1-2 Expression of *Gcm2* and *Foxn1* during parathyroid glands and thymus development in E4.5 chick embryos.** *In situ* hybridisation and corresponding schemes of *Gcm2* **(A, B)** and *Foxn1* **(C, D)** expression in 3/4 PP endoderm. A, Anterior; D, Dorsal; PP, Pharyngeal Pouch; P, Posterior; V, Ventral. Adapted from Neves et al., 2012.

The thymus organogenesis occurs in two distinct temporal phases: a thymocyte-independent phase followed by a thymocyte-dependent phase (Rodewald, 2008). In the first one, cellular interactions between the PP endoderm and the surrounding NC-derived mesenchyme drive the specification of TECs. In chick, one report showed that the failure of sufficient quantities of cephalic neural crest cells (cNCCs) to migrate and interact with these developing organs results in ectopic, hypoplastic or absent thymic lobes. Moreover, reduced or absent parathyroids in at least one side of the embryo are also observed (Bockman and Kirby, 1984). *Pax3* knockout-mice, with severe NCC deficiency show large thymus and small parathyroid glands rudiments, and these organs fail to detach from the pharynx and from each other (Griffith et al., 2009).

The importance of the epithelial-mesenchymal interactions during thymus organogenesis was first demonstrated in 1967 by Le Douarin using the quail-chick chimera system. Quail endoderm isolated from the 3/4PP was able to develop into functional TECs when associated with a chicken permissive mesenchyme (somatopleura), but not when associated with a non-permissive mesenchyme (limb bud). In fact, permissive ectopic mesenchymal tissues are able to mimic the role played by neighbouring NC-derived mesenchyme in thymus development (N. Le Douarin, 1967). This endoderm-mesenchyme crosstalk was recently explored and it was shown that a specific spatial-temporal expression of BMP and FGF factors is fundamental for endoderm development and specification into TECs (Neves et al., 2012). Additionally, a transcription-factor network involving the expression of *Hoxa3* (Manley and Capecchi, 1995), *Pax1/9* (Wallin et al., 1996; Peters et al., 1998; Hetzer-Egger et al., 2002), *Eya1* and *Six1* (Xu et al., 2002) is crucial for normal thymus organogenesis in mouse.

In the later stage of thymus development, the thymocyte-dependent phase, maturation of the thymic epithelium in cTECs and mTECs compartments, is driven by the initial colonization by LPCs, at E6.5 in chicken (Le Douarin and Teillet, 1973; Douarin and Jotereau, 1975) and at E11.5 in mouse (Owen and Ritter, 1969; Fontaine-Perus et al., 1981). This LPCs colonization and further maturation steps of TECs are dependent on the

expression of *Foxn1* by TECs (Nehls et al., 1996). Several reciprocal signals between thymocytes and immature TECs induce co-differentiation of T lymphocytes and TECs (Alves et al., 2009). In this context, Notch signaling has been subject of study, since both ligands and receptors are co-expressed in the TECs and developing thymocytes (Anderson and Jenkinson, 2001; Parreira et al., 2003).

### 1.4. Notch signaling

Notch signaling is a fundamental signaling-pathway that mediates cell-cell communication during animal development. It regulates cell proliferation, fate, survival and differentiation in all metazoans (Kopan, 2012; Greenwald and Kovall, 2013), in a dose-, timing- and context-dependent fashion (Maillard et al., 2005). Specifically, it has been implicated in the control of several aspects of organogenesis such as bone development (Watanabe et al., 2003), function and neural development (Hitoshi et al., 2002), angiogenesis (Liu et al., 2003), somitogenesis (Conlon et al., 1995) and haematopoiesis (Jaleco et al., 2001; Parreira et al., 2003; Neves et al., 2006; Alcobia et al., 2011; Laranjeiro et al., 2012).

Notch receptors (Notch1-2 in birds and Notch1-4 in mammals) bind to five different ligands [Delta-like1, 3 and 4, and Serrate1-2 (Jagged1-2 in mammals)] present in the adjacent cells (Bray, 2006), leading to the cleavage and release of the intracellular domain of Notch (ICN) by the γ-secretase complex (Kopan, 2012). ICN is then translocated into the nucleus where it binds CSL, a transcription factor that mediates most of the well-characterized Notch functions. This binding furthers the recruitment of other transcriptional activators, like the co-activator protein Mastermind-like (MAML), thereby activating the transcription of many downstream target genes, such as the basic helix-loop-helix (bHLH) *Hes* genes (Kopan and Ilagan, 2009) (**Figure 1-3**). *Hes* genes are the mammalian homologs of the *Drosophila* genes *Hairy* and *Enhancer of Split*, and function as effectors of Notch signaling. It has been shown their importance as biological clocks, measuring time in development events such as somite segmentation, and in the regulation of binary cell fate decisions in the developing nervous system of mouse embryos (Kageyama et al., 2007).

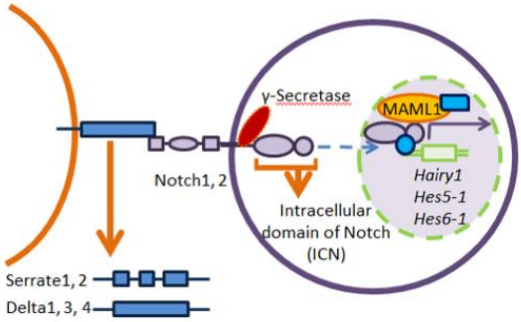


**Figure 1-3 Schematic representation of Notch signaling pathway in birds.** Serrate or Delta ligands bind to the Notch receptor, leading to the proteolytic cleavage of the ICN by γ-secretase. ICN enters the nucleus, binds to co-activators such as MAML1, and activates the transcription of Notch target genes (*Hairy*, *Hes5.1* and *Hes6.1*).

### 1.5. Notch signaling in thymus and parathyroid organogenesis

Several evidences point out to important roles of Notch signaling in haematopoiesis and lymphopoiesis. The expression of Notch-related genes in the adult thymus was demonstrated for the first time by Parreira et al. (2003), suggesting the involvement of Notch signaling in thymic function. The generation of the earliest haematopoietic stem cells (Radtke et al., 2010) and the expansion and lineage-differentiation of early-myeloid progenitors (Neves et al., 2006) were shown to be Notch-dependent. In fact, it was shown that Notch ligands Delta1 (Jaleco et al., 2001) and Delta4 (Koch et al., 2008) are responsible for T/B lineage decision and promote the development of the thymocytes into T lymphocytes (Jiang et al., 1998; Jiménez et al., 2001; Fiorini et al., 2009). Recent studies report a role of thymocytes to provide Notch signals to TECs, stressing its importance in the regulation of late thymic organogenesis (Koyanagi et al., 2012). It is known that the lack of Jagged2 has a negative impact in the medullar organization of the thymus (Jiang et al., 1998), and that the presence of Delta1 is necessary for the development of both cTECs and mTECs (Masuda et al., 2009). Additionally, the maintenance of a high proliferative potential of the thymic epithelial stem cells by ΔNp63 (a particular isoform of p63) is dependent on the presence of Jagged2 as a downstream effector (Candi et al., 2007).

Nevertheless, only few recent evidences point to the role of Notch signaling in the early stages of thymus and parathyroid glands organogenesis. In chicken development, the expression of Notch-related genes (receptors, ligands and target genes) in the endoderm of the 3/4 PP and surrounding mesenchyme at E4, provided the first evidence of an active Notch signaling in the prospective thymus and parathyroid domains. Moreover, preliminary data of *in vitro* inhibition of Notch signaling specifically in the pharyngeal region, showed a blockage or reduction of the *Gcm2* expression while *Foxn1* expression appears to be randomly affected (Figueiredo, 2011).

In order to understand the *very* beginning of avian thymus and parathyroid glands organogenesis we aim to study the role of Notch signaling during their early phases of development.

### 1.6. Objectives

The aim of this project was to unravel the role of Notch signaling during the early stages of the avian thymus and parathyroid glands organogenesis. Two distinct approaches were performed in order to manipulate Notch signaling: pharmacological inhibition and gain- and loss-of-function of Notch signaling by genetic manipulation of tissues. With regard to this, two strategies involving two embryological sources of the prospective domains of the thymus and parathyroid glands (3/4PP endoderm) were used in an organotypic *in vitro* system:

1) Explants of the pharyngeal region of E3 quail embryos. With this strategy, the 3/4 PP endoderm is in close contact and preserve 3D interactions with local tissues (mesenchyme and ectoderm);
2) Heterospecific associations of isolated 3/4 PP endoderm with ectopic permissive mesenchyme (somatopleura) (developed by Neves et al, 2012);

In the first approach (1), the pharyngeal region explants were grown in the presence of two distinct γ-secretase inhibitors, DAPT and LY411575, to test the effect of Notch signaling inhibition in the tissues involved in epithelial-mesenchymal interactions during early thymic and parathyroid glands organogenesis.

In the second approach (2), heterospecific associations of isolated quail 3/4 PP endoderm with chicken somatopleural mesenchyme were first grown in the presence of DAPT, similar to described above. Secondly, quail 3/4 PP endoderm was genetically modified in a cell-autonomous manner (with gain- and loss-of-function of Notch signaling) and associated in culture with chicken somatopleural mesenchyme. With this approach, we tested the effects of Notch signaling modulation in the prospective domains of the thymus and parathyroid glands during epithelial-mesenchymal interactions at early-stages of organs formation. In this context, a new construct for the loss-of-function experiments (pT2K-NLS-Cherry-DNMAML1eGFP) was generated.

Quantitative Real-Time PCR (qRT-PCR) analysis was performed in both experimental approaches. Notch activity was then evaluated by the expression of the Notch target gene *Hes5.1*, and thymus and parathyroid glands formation by *Foxn1* and *Gcm2* expression, respectively.

## 2. EXPERIMENTAL DESIGN TO MODIFY NOTCH SIGNALING

### 2.1. Pharmacological Notch signaling inhibition

γ-secretase complex has a key role in the Notch signaling pathway, allowing the cleavage and release of ICN and its import into the nucleus. By inhibiting γ-secretase activity, we were able to block Notch signaling and evaluate the effects in the early stages of the avian thymus and parathyroid glands organogenesis. Two cell permeable γ-secretase pharmacological inhibitors were used: DAPT (N-S-phenyl-glycine-t-butyl ester; Dovey et al., 2001) and LY411575 (a DAPT analogue; Fauq et al., 2007). LY411575 is structurally similar to DAPT, but 100-fold more potent.

### 2.2. Genetic modification with gain- and loss-of-function of Notch signaling

It is known that cells forced to express the intracellular domain of Notch1 (ICN1) have a constitutive activation of Notch signaling in a ligand-independent manner (Weinmaster, 1997). Conversely, cells forced to express a dominant-negative (DN) form of the co-activator Mastermind-like1 (DNMAML1), consisting only in the N-terminal binding domain, block Notch signaling probably due to an inability of this truncated protein to recruit other proteins of the Notch transcriptional activation complex (Maillard et al., 2004).

To genetically modify Notch signaling in avian tissues we used a system of vectors combining a *Tol2*-mediated gene transfer technique and a Tetracycline-dependent conditional gene expression (Sato et al., 2007; Watanabe et al., 2007) (**Figure 2-1**). The system of vectors comprises three different plasmids: pT2K-CAGGS-tTA, constitutively expressing a tetracycline-controlled transcriptional activator (tTA); pT2K-BI-TREeGFP, a plasmid containing a cassette in which two different genes can be bidirectionally transcribed under the control of a tetracycline-responsive element (TRE), and pCAGGS-T2TP, a transposase that allows the stable integration of the two former plasmids. Upon integration in the host genome, and in the absence of Doxycycline (Dox) (a tetracycline analogue), tTA gene product will bind to the promoter cis-element TRE, activating the TRE-driven genes. By adding Dox to the culture medium, tTA is released from TRE, shutting off the expression of the TRE-driven genes (Tet-off expression system). *ICN1* and *DNMAML1* sequences were previously cloned in pT2K-BI-TREeGFP generating pT2K-ICN1eGFP and pT2K-DNMAML1eGFP (Figueiredo, 2011), respectively. A new construct with *DNMAML1* fused to *CherryNLS* sequence, pT2K-NLS-Cherry-DNMAML1eGFP, was generated to improve protein stability and nuclear translocation of DNMAML1:

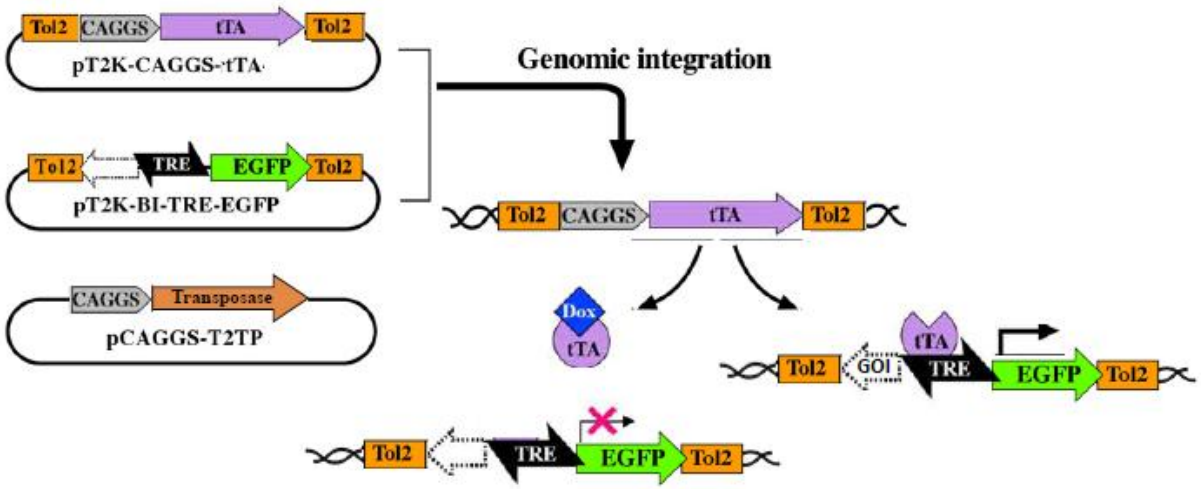


**Figure 2-1 Schematic representation of the *Tol2*-mediated gene transfer technique and Doxycycline-dependent switch-on/off of gene expression.** Transient activity of transposase (pCAGGS-T2TP) induces the integration in the host genome of either transactivator (pT2K-CAGGS-tTA) or TREeGFP (pT2K-BI-TREeGFP). In the absence of doxycycline, the product of the gene tTA (transactivator) activates the transcription of the TRE-driven genes: gene of interest (GOI) or EGFP. Adapted from Sato et al., 2007.

## 2.3. Materials and methods

### 2.3.1 Chemically competent cells preparation

Since *E. coli* cells are not naturally competent, they need to undergo a process that make them able to uptake exogenous DNA. Non-competent cells of the DH5α strain were inoculated in LB plates and grown overnight at 37ºC. One single colony was selected, inoculated in 3mL of LB medium and left overnight in a 37ºC shaker (220rpm). 2mL of this grown culture were added to 200mL of LB medium and incubated for 3h under the same conditions until $OD_{600}$=0.4-0.6. From then on, all steps were performed on ice, refrigerated centrifuges and using cold solutions. Cells were initially centrifuged at 4000rpm for 5min at 4ºC and the supernatant was discarded. Half of the initial bacterial culture volume of $MgCl_2$ 0.1M was added, cells were again centrifuged and supernatant removed. Half of the initial bacterial culture volume of $CaCl_2$ 0.1M was then added and cells were incubated on ice for 30min. After another centrifugation, supernatant was discarded and cells were carefully resuspended in $CaCl_2$ 0.1M/15% Glycerol to 1/15 of the initial volume. The final cell suspension was aliquoted in 500µL sterile cryovials and stored at -80ºC.

### 2.3.2 Transformation

All the *E. coli* DH5α transformations were performed by adding 100-500ng of plasmid DNA to 200µL of competent cells. After gently mixing, the mixture stayed on ince for 30min. A heat shock was performed for 1min at 42ºC, followed by 2min of incubation on ice. 600µL of LB medium was added to the cells and incubation in a 37ºC shaker (220rpm) for 1h enabled the expression of the ampicillin resistance gene (*bla*). After that, cells were centrifuged at 5000g for 3min. 650µL of the supernatant were discarded and cells were resuspended on the remaining 150µL. Finally, the 150µL of cells were plated on LB Agar supplemented with ampicillin (100µg/mL) (Sigma) and incubated overnight at 37ºC.

### 2.3.3 Cell growth, plasmid purification and cell banks

Single colonies of DH5α transformed with each plasmid were collected and added to 5mL of LB medium supplemented with 5µL of ampicillin (100µg/mL) in a 50mL. For small scale plasmid extraction, cells were grown overnight in a 37ºC shaker (220rpm). The purification of plasmid DNA was carried out using QIAprep®Spin Miniprep Kit (QIAGEN) according to the recommended protocol. For midi-preparation of plasmid DNA, cells were incubated for 7-8h (37ºC, 220rpm). Then, 1mL of this pre-culture was added to 50 or 100mL (high- or low-copy plasmids, respectively) of LB medium supplemented with ampicillin (100µg/mL) in a 250 or 500mL erlenmeyer. Cultures were left to grow overnight at 37ºC at 220rpm. The plasmid DNA purification was performed using QIAfilter Plasmid Midi Kit (QIAGEN) according to the manufacturer's instructions. DNA concentration and purity were determined using

NanoDrop® ND-1000 Spectrophotometer (Thermo Scientific) and samples were stored at -20ºC.

For each new plasmid, a working cell bank was always performed by adding 150µL of the pre-culture to 850µL of glycerol 100% in a sterile 2mL eppendorf and storing at -80ºC.

2.3.4 Generation of pT2K-NLS-Cherry-DNMAML1eGFP

To improve protein stability of DNMAML1 and its nuclear translocation we cloned the *DNMAML1* sequence in fusion with the *CherryNLS* sequence in pT2K-BI-TREeGFP plasmid.

2.3.4.1 PCR amplification

DNMAML1 is the dominant negative form of MAML1 and corresponds only to its 12-74aa (36-224 nucleotides) in *Gallus gallus*. The nucleotide sequence of *DNMAML1 Gallus gallus* is shown below (primers location in bold):

MAML1 Gallus gallus ID: XM_414607.2

1 atggtgctgc ccccctgccc catggcccat tta**gtggtgc cgcggcacag c**gcggtgatg

61 gagcggccct ttcagcgcat cgagctctgc cggcggcacc acagcgcctg cgagtcccgc

121 taccaggccg tgtccccgga gcgcctggag ctggagcgcc agcaaacctt cgccctgcac

181 cagcgctgcc tgcaggccaa gg**ccaagcgg gccggcaagc ac**cgccagcc gcccccggcc

...

To amplify *DNMAML1* and allow its cloning and further expression, a forward primer from a previous work (Figueiredo, 2011), that was modified to introduce a *NheI* restriction site (bold) and a KOZAK sequence (underlined), was used: 5´**GCTAGC**CATGgtggtgccgcggcacagc 3'. The reverse primer was also modified introducing an *EcoRV* restriction site (bold): 5'**GATATC**gtgcttgccggcccgcttggc 3'. Inserted sequence is in capital letters.

Cherry is a fluorophore with high photostability and rare fluorescence-intensity fluctuations (Seefeldt et al., 2008) and was used as a tag for *DNMAML1* in this work. *Cherry* carrying a nuclear localization signal (NLS) was cloned in a pCAG plasmid (pCAG-CherryNLS; Vilas-Boas et al., 2011) and its partial nucleotide sequence is shown below (primers location in bold):

1 **atggtgagca agggcgagga g**gataacatg gccatcatca aggagttcat gcgcttcaag

61 gtgcacatgg agggctccgt gaacggccac gagttcgaga tcgagggcga gggcgagggc

121 cgcccctacg agggcaccca gaccgccaag ctgaaggtga ccaagggtgg ccccctgccc

181 ttcgcctggg acatcctgtc ccctcagttc atgtacggct ccaaggccta cgtgaagcac

...

661 cgcgccgagg gccgccactc caccggcggc atggacgagc tgtaccctcc aaaaaagaag

721 agaaa**ggtag aagacccctg attgtaca**

To amplify *CherryNLS* and allow direct cloning in fusion with *DNMAML1* sequence in pT2K-DNMAML1eGFP plasmid, both forward and reverse primers were modified to introduce an *EcoRV* restriction site (capital and bold letters). The final primers used were: forward 5'**GATATC**atggtgagcaagggcgaggag 3' and reverse 5'**GATATC**tgtacaatcaggggtcttctacc 3'.

*DNMAML1* sequence was amplified from 10ng of TOPO-DNMAML1 vector from a previous work (Figueiredo, 2011) and *CherryNLS* from 10ng of pCAG-CherryNLS plasmid, both in a 25µL PCR reaction using Phusion™ Master Mix with HF Buffer (Finnzymes) and 0.5µM final concentration of the primers described above, according to manufacturer's instructions. The cycling conditions were: 1 cycle of initial denaturation at 98ºC for 30sec; 30 cycles of denaturation at 98ºC for 10sec, annealing at 65ºC for 30sec, and extension at 72ºC for 15sec/Kb (205bp product for *DNMAML1* and 761bp product for *CherrryNLS*); a final extension cycle at 72ºC for 10min. All PCR reactions were performed in a MyCycler™ Thermal Cycler (Bio-Rad), and PCR products were resolved on a 1.5% agarose gel (see section 2.3.10) and stored at -20ºC.

2.3.4.2 TOPO II PCR Cloning

*DNMAML1* and *CherryNLS* PCR products were cloned in pCR®II-TOPO® vector using TOPO TA Cloning® Kit (Invitrogen) according to the manufacturer's instructions. In order to add single 3' adenine overhangs to the PCR products, they were previously incubated at 72ºC for 10min with 0.25µL of Go-Taq Polymerase. TOPO® Cloning reactions were transformed into One Shot® MAX Efficiency® DH5α-T1$^R$ Chemically competent *E. coli* cells (Invitrogen) according to the instructions. Four white colonies of each plasmid were chosen and plasmid DNA was extracted using QIAprep®Spin Miniprep Kit (QIAGEN) as described (see section 2.3.3). The presence of the insert was then confirmed by restriction analysis (see section 2.3.4.3).

2.3.4.3 Restriction analysis

To confirm the presence of *DNMAML1* and *CherryNLS* in each vector, digestions with restriction enzymes were performed. For *DNMAML1* we did a double digestion with *NheI* (New England Biolabs - NEB) and *EcoRV* (Promega) using Buffer 2 from NEB (10mM Tris-HCl pH7.9, 10mM MgCl2, 50mM NaCl and 1mM DTT). For *CherryNLS* a single digestion with *EcoRV* (Promega) using Buffer D from Promega (6mM Tris-HCl pH7.9, 6mM MgCl2, 150mM NaCl and 1mM DTT) was done. These digestions were performed in 4000ng of total plasmid DNA and 20µL final volume and were incubated for 2h30min at 37ºC. Digestion results were analysed by agarose gel electrophoresis (see section 2.3.10).

#### 2.3.4.4 Cloning *DNMAML1* in pT2K-BI-TREeGFP

##### 2.3.4.4.1 Double digestion with restriction enzymes and purification

After confirming the TOPO-DNMAML1 and TOPO-CherryNLS clones, the first step was to clone *DNMAML1* in pT2K-BI-TREeGFP. 2µg of pT2K-BI-TREeGFP and 8µg of TOPO-DNMAML1 were double digested with *NheI* and *EcoRV*, as previously described, in a final reaction volume of 30µL and 80µL, respectively. Digestion product of pT2K-BI-TREeGFP was purified using the QIAquick PCR Purification Kit (QIAGEN) according to the instructions. Digestion products of TOPO-DNMAML1 and TOPO-CherryNLS were loaded on a 1.5% agarose gel (see section 2.3.10) and the fragments of interest were collected and purified using QIAquick Gel Extraction Kit (QIAGEN) according to the manufacturer's instructions. In both cases, DNA was eluted in 30µL of EB Buffer.

##### 2.3.4.4.2 Ligation reaction and transformant analysis

Ligation reaction between pT2K-BI-TREeGFP and *DNMAML1* was performed according to the correlation *ng of insert = ((ng of vector x Kb size of insert)/Kb size of vector) x 10*. Thus, 150ng of pT2K-BI-TREeGFP (8,7Kb) were added to 35ng of DNMAML1 (0,2Kb), using 1µL of T4 DNA Ligase (NEB 400U/µL) and the correspondent 1X Buffer (50mM Tris-HCl pH7.5, 10mM MgCl2, 1mM ATP and 10mM DTT) in a final volume of 20µL, at room temperature (RT), overnight. Half of the ligation result was used to transform DH5α cells as described (see section 2.3.2). Transformants were tested for the presence of the recombinant plasmids of interest by repeating the procedures 2.3.3 and 2.3.4.3.

#### 2.3.4.5 Cloning *CherryNLS* in pT2K-DNMAML1eGFP

After confirming the presence of *DNMAML1* in pT2K-DNMAML1eGFP, the *CherryNLS* sequence was fused to *DNMAML1*. 2µg of pT2K-DNMAML1eGFP and 4µg of TOPO-CherryNLS were digested with *EcoRV* and purified as described in section 2.3.4.4.1. Before the ligation reaction, the linearized pT2K-DNMAML1eGFP was dephosphorilated in order to prevent auto-ligation by adding 1X CIP enzyme and 1X Buffer 3 from NEB (50mM Tris-HCl pH7.9, 10mM MgCl2, 100mM NaCl and 1mM DTT), and incubated at 37ºC for 3h. After a new purification step (see 4.4.1), the ligation reaction between *CherryNLS* and pT2K-DNMAML1eGFP was performed by adding 150ng of vector (8,9Kb) to 13ng of insert (0,76Kb) in the same conditions described in 2.3.4.4.2. After purification and quantification steps, the correct orientation of the insert in pT2K-DNMAML1eGFP was confirmed by agarose gel electrophoresis (see section 2.2.10) after restriction analysis with *PvuII* using Buffer B from Promega (6mM Tris-HCl pH7.5, 6mM MgCl2, 50mM NaCl and 1mM DTT).

2.3.5 Avian Embryos

Fertilised chicken eggs (*Gallus gallus*) were obtained from Sociedade Agrícola Quinta da Freiria, S.A., Portugal, and Japanese quail eggs (*Coturnix coturnix japonica*) from Interaves, Sociedade Agro-Pecuária, S.A., Portugal. Eggs were stored at 16ºC and incubated at 38ºC to initiate development. Dissection was performed at specific stages according to Hamburger and Hamilton stages (HH, Hamburger and Hamilton, 1951) or after distinct incubation times.

2.3.6 Organotypic assay of explants of the pharyngeal region

The pharyngeal region between the first and fourth PA was dissected from quail E3 embryos, cut dorsally along the anterior/posterior axis (along the notochord), and kept in PBS and on ice until culture setting. Explants were cultured with the opened dorsal side down, placing endodermal tissues in contact with the 74µm Mesh Size Polyester Membrane (24mm Netwell™ , Corning) and in culture medium (**Figure 2-2**) for 48h in a humidified incubator at 37ºC with 5% $CO_2$. Culture medium was RPMI-1640 (Sigma) supplemented with 10% Fetal Bovine Serum (FBS) (Invitrogen) and 1x Pen/Strep.

For Notch signaling inhibition, two distinct pharmacological inhibitors were used: DAPT – InSolution™ γ-Secretase Inhibitor IX (Calbiochem), and Stemolecule™ LY411575 (Stemgent). Culture medium was supplemented with different concentrations of the two inhibitors: 12.5, 25, and 50µM for DAPT; or 100 and 200nM for LY411575.

The control culture medium was supplemented with DMSO (Sigma) at the concentration used in the corresponding experimental condition (with γ-Secretase inhibitor), and a dose-response curve was performed to check for toxic concentrations (see **Table 2-1**).

**Table 2-1** DMSO concentrations used to perform the dose-response curve and the respective inhibitors (DAPT and LY411575) concentrations.

| **DAPT** | |
|---|---|
| **Inhibitor (µM)** | **DMSO concentration** |
| **12.5** | 0.05% |
| **25** | 0.1% |
| **50** | 0.2% |
| **-** | 0.4% |
| **-** | 0.8% |
| **LY411575** | |
| **Inhibitor (nM)** | **DMSO concentration** |
| **100** | 0.1% |
| **200** | 0.2% |

After 48h of culture, explants were washed in PBS, RNA extracted (see section 2.3.8.2) and qRT-PCR analysed (see section 2.3.9). For each culture condition, a pool of two to five samples replicates (n=2-5) was obtained for qRT-PCR analysis. Each sample consisted of a pool of five pharyngeal explants. Freshly dissected pharyngeal regions (E3) were used to evaluate gene expression analysis at 0h of culture. In vitro assays were performed in collaboration with Marta Figueiredo, the PhD student from our research team.

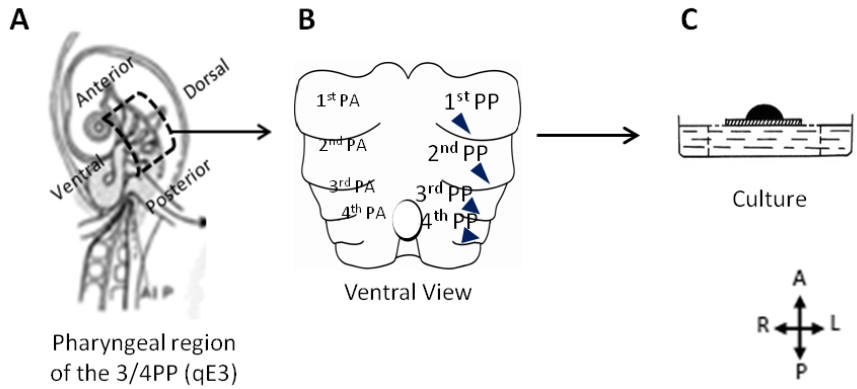


**Figure 2-2 Schematic representation of the *in vitro* culture of the pharyngeal region explants.** Region of the pharynx dissected at E3 quail embryo **(A)**. Ventral view of the dissected pharyngeal region **(B)**. Pharyngeal explants are grown in the presence (experimental condition) or absence (control condition) of the pharmacological inhibitors of Notch signaling. Note the PP endoderm in contact with the culture medium **(C)**. A, Anterior; D, Dorsal; PA, Pharyngeal Arch; PP, Pharyngeal Pouch; P, Posterior; V, Ventral.

### 2.3.7 Organotypic assay of heterospecific association of tissues

The region of the 3rd and 4th PA was dissected from quail embryos at E3 (HH-stage 21) and treated with a solution of pancreatin (25g/L, Sigma) for 60-90min on ice to allow the separation of the endoderm from the pharyngeal mesenchyme and ectoderm. Somatopleural mesenchymal tissues of E2.5 chick embryos (HH-stage 18) were isolated at the level of somites 19 to 24. The mesenchyme was further treated with a solution of pancreatin (25g/L, Sigma) for 10-20min on ice to allow its dissociation from endodermal and ectodermal tissues. Isolated 4-5 endodermal explants were associated with 4-5 mesenchymal explants on Nucleopore membrane filters (Millipore) supported by fine meshed metal grids (Goodfellows), placed in culture dishes and in contact with culture medium [RPMI-1640 (Sigma) supplemented with 10% Fetal Bovine Serum (FBS) (Invitrogen), 1x Pen/Strep], for 48h in a humidified incubator at 37ºC with 5% $CO_2$. After 48h, cultured tissues were washed in PBS, RNA extracted (see section 2.3.8.2) and qRT-PCR analysed (see section 2.3.9). Freshly dissected endodermal and mesenchymal explants (E3) were used to evaluate gene expression at 0h of culture. In vitro assays were performed in collaboration with Marta Figueiredo, the PhD student from our research team.

#### 2.3.7.1 Notch signaling inhibition by DAPT

For Notch signaling inhibition, a pharmacological inhibitor was used: DAPT – InSolution™ γ-Secretase Inhibitor IX (Calbiochem). The culture medium [RPMI-1640 (Sigma) supplemented with 10% FBS (Invitrogen), 1x Pen/Strep] was supplemented with 50µM of DAPT – InSolution™ γ-Secretase Inhibitor IX (Calbiochem). The control culture medium was supplemented with 0.2% DMSO (Sigma) (see **Table 2-1**).

2.3.7.2 Notch signaling modulation by genetic modification of the endodermal tissues

Isolated quail 3/4PP endoderm was genetically modified by electroporation (250V, 500µF in PBS) using distinct combination of the above described tetracycline-dependent system of vectors (**Figure 2-1**): no vectors (control condition), 30µg of pT2K-BI-TREeGFP (vector control condition); 30µg pT2K-ICN1eGFP (gain-of-function condition); 30µg pT2K-DNMAML1eGFP (1st loss-of-function condition) or 30µg pT2K-NLS-Cherry-DNMAML1eGFP (2nd loss-of-function condition). For all vector conditions 15µg of pT2-CAGGS-tTA (transactivator) was added. For these experiments, we did not use the transposase vector due to the short period of culture time. These experiments were performed using the transient effect of electroporated vectors. After electroporation, the endodermal tissues were kept in 100% FBS (Invitrogen) for 5-10min, on ice.

For each condition, 4-5 electroporated endodermal explants were associated with 4-5 mesenchymal explants and grown for 48h, as previously described (see section 2.3.7).

2.3.8 RNA isolation and Reverse Transcription

2.3.8.1 RNA isolation from samples for qRT-PCR calibration curves

Quail E9 embryos were dissected and thymi and parathyroid glands were separately isolated. Chicken E18 embryos were as well dissected to isolate thyroid glands. An OP9 cell line carrying a plasmid to express GFP (OP9-GFP; Schmitt, 2002) was also subjected to RNA isolation. Total RNA from chicken or quail organs (thymus, parathyroid and thyroid) and OP9-GFP cell line was extracted using High Pure RNA Isolation Kit (Roche) according to the manufacturer's instructions. Samples were DNase digested for 40min and RNA was eluted in 50µL of Elution Buffer.

2.3.8.2 RNA isolation from organotypic assays

Total RNA from the samples was extracted using a combination of TRIzol reagent (Invitrogen) and RNeasy Mini Kit (QIAGEN) manufacturer's instructions. To each sample, 1mL of Trizol was added and they were then maintained at -80ºC until RNA extraction. After thawing at RT, 200µL of chloroform were added. Tubes were vigorously shaken for 15sec, allowed to stand 10min at RT and centrifuged at 13000rpm for 15min at RT. Aqueous (colorless) phase, avoiding organic pahse, was withdrawn to a clean eppendorf and ethanol precipitation of RNA was performed as described on the RNeasy Mini Kit protocol. DNase digestion was carried out for 15min and RNA was eluted in 50µL of RNase-free water. All RNA samples were stored at -80ºC.

2.3.8.3 Reverse transcription

First-strand cDNA synthesis was performed in a total volume of 20µL, by reverse transcription of 2µg of total RNA using the SuperScript™ III Reverse Transcriptase kit and

Oligo $(dT)_{12-18}$ Primer (Invitrogen), according to the manufacturer's instructions. Synthesized cDNAs were stored at -20ºC. All steps of RNA extraction and cDNA synthesis were performed in a vertical laminar flow hood.

Concentration and purity of both the RNA and cDNA samples were determined using the NanoDrop® ND-1000 Spectrophotometer (Thermo Scientific).

2.3.9 Quantitative Real-Time PCR

Specie-, organ- and construct-specific primers were designed and tested and qRT-PCR assays were optimized. Primers were designed either by using Primer3 software or manually (list in

**Table 6-1**). Except for *qGAPDH*, *DNMAML*, *ICN1* and *GFP*, primer pairs were designed to be intron-spanning (to exclude amplification of genomic DNA) and near 3'poly-A. qRT-PCR assays were run in a 7500 Fast Real-Time PCR System (Applied Biosystems) in MicroAmp® Fast Optical 96-Well Reaction Plate (Applied Biosystems). Reactions were performed in 25µL volume using 12.5µL of Power SYBR® Green PCR Master Mix (Applied Biosystems), 0.4µM final concentration of primers and 1µL of cDNA. Thermocycling conditions were composed by an initial denaturation at 50ºC for 20sec and 95ºC for 10min, followed by 40 cycles at 95ºC for 15sec and at specific annealing temperature (see

**Table 6-1** and **Table 6-2**) for 1min. To assess amplification efficiency, and as a positive control, a calibration curve for each gene was performed using 10-fold dilutions of a sample that was known to express the gene of interest (see **Table 6-2**). To control primers specificity, at the end of each experiment a melting curve was generated by increasing the temperature from 60ºC to 95ºC. Relative quantification of gene expression was determined by the ΔΔCt method (Livak and Schmittgen, 2001), of by the Pfaffl method (Pfaffl, 2001) using quail Glyceraldehyde-3-phosphate dehydrogenase (qGAPDH) as endogenous control gene to normalize the variability in expression levels. To discriminate quail and chicken tissues in the experiments of heterospecific association of tissues, qGAPDH primer pair was designed (and further tested) to specifically amplify quail GAPDH but not chicken GAPDH. All the experiments were carried out in a horizontal laminar flow hood to avoid contamination and using two biological replicates for each condition.

2.3.10 Agarose gel electrophoresis

Analysis of RNA and DNA integrity, purification of specific DNA segments and confirmation of PCR amplification products as well as digestion results were performed using agarose gel electrophoresis. UltraPure™ Agarose (Invitrogen) was dissolved in 1X TAE to a final concentration of 0.8-1.8%, according to the DNA fragments size. GelRed™ Nucleic Acid Gel Stain, 10,000X in DMSO (Biotium) was used as intercalating agent and added to the gel at 1:10,000. 6X Loading Dye Solution (Fermentas) diluted 6 times was added to each sample

according to the final volume and the gel was loaded. According to the expected fragment sizes FastRuler™ DNA Ladder Low Range, FastRuler™ DNA Ladder Middle Range or O'GeneRuler™ 1 kb DNA Ladder (Fermentas) were used. Electrophoresis was run in 1X TAE at 5-10V/cm of gel length, results were seen on a UV transilluminator and images were acquired with ChemiDoc™ XRS+ (Bio-Rad) and Image Lab 4.1 software.

## 3. RESULTS

### 3.1. Pharmacological inhibition of Notch signaling in pharyngeal region explants.

To unravel the role of Notch signaling during epithelial-mesenchymal interactions in early-organogenesis of the thymus and parathyroid glands, we started to perform an *in vitro* loss-of-function of Notch signaling using two distinct pharmacological inhibitors of γ-secretase activity: DAPT and LY411575. Different concentrations of the distinct inhibitors DAPT (12.5, 25 and 50µM) or LY411575 (100 and 200nM) were used in cultures of pharyngeal region explants (quail E3). After 48h of culture, Notch signaling inhibition was evaluated by the expression of Notch target gene *Hes5.1*, and its effects in thymus and parathyroid glands organogenesis by *Foxn1* and *Gcm2* expression, respectively. Gene expression was quantified using Quantitative Real-Time PCR analysis.

As the distinct inhibitors were reconstituted in DMSO, we began to evaluate the toxicity effect of DMSO in cultured tissues. For that, we quantified the expression of *Foxn1*, *Gcm2* and *Hes5.1* in distinct DMSO concentrations (from 0 to 0.8%, see **Table 2-1**).

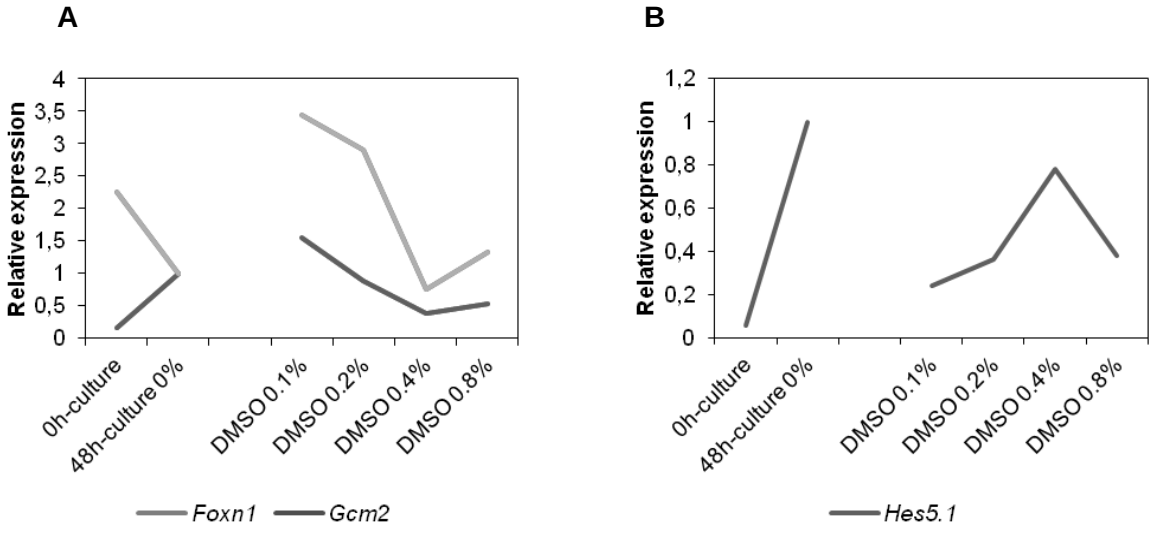


**Figure 3-1** Relative expression of *Foxn1* and *Gcm2* **(A)**, and *Hes5.1* **(B)** at 0h (E3), and after 48h of culture in the distinct DMSO concentrations (from 0% to 0.8%). 0h-culture, n=3; 48h-culture, n=2; all DMSO samples, n=5.

Before culture (0h), the initial expression of *Foxn1*, *Gcm2* and *Hes5.1* was evaluated in freshly isolated pharyngeal region explants (E3). As shown in **Figure 3-1**, low expression of

*Foxn1* and *Hes5.1* was observed, when compared to the strong *Gcm2* expression at this time of development. After 48h of culture, pharyngeal explants grown without DMSO (control) had an increased expression of *Foxn1* (**Figure 3-1 A**) and *Hes5.*1 (**Figure 3-1 B**), while *Gcm2* (**Figure 3-1 A**) expression was reduced when compared to 0h-culture.

When the explants were grown for 48h with increasing doses of DMSO, a fluctuation of *Foxn1*, *Gcm2* and *Hes5.1* expression was observed. At lower doses of DMSO (0.1% and 0.2%), the highest expressions for *Foxn1* and *Gcm2* were observed while accompanied by a strong reduction of *Hes5.1* expression (**Figure 3-1**). Moreover, explants grown with 0.4% of DMSO presented a 60% reduction of *Foxn1* expression (**Figure 3-1**). These results define the toxicity effect of DMSO at doses ≥ 0.4% DMSO. Consequently, all experimental conditions using Notch signaling inhibitors were performed using <0.4% of DMSO.

3.1.1 DAPT:

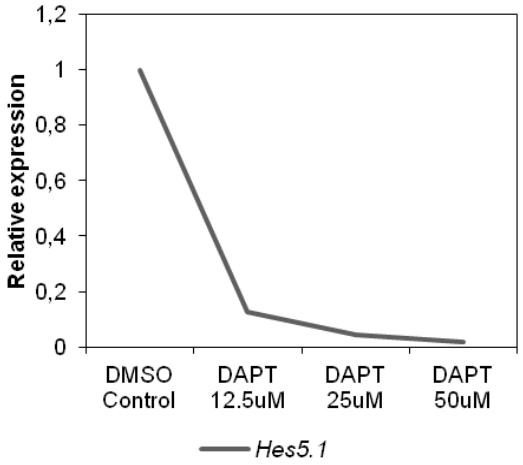


**Table 3-1** *Hes5.1* **e**xpression in the pharyngeal region explants.

| *Hes5.1* | Average | StDev | p-value |
|---|---|---|---|
| DMSO Control | 1,000 | - | - |
| DAPT 12.5μM | 0,128 | 0,049 | 0,005 |
| DAPT 25μM | 0,043 | 0,010 | 0,017 |
| DAPT 50μM | 0,019 | 0,017 | 0,025 |

**Figure 3-2** Relative expression of *Hes5.1* in the pharyngeal region explants grown at increased concentrations of DAPT. 5 samples for each culture conditions.

When the pharyngeal region explants were grown in the presence of 12.5μM (0.05% DMSO), 25μM (0.1% DMSO) and 50μM (0.2% DMSO) of Notch inhibitor DAPT, we observed a significant decrease of *Hes5.1* expression when compared with the respective control conditions (only DMSO) (**Figure 3-2** and **Table 3-1**). Moreover, this decrease of *Hes5.1* expression was also dose-dependent (**Table 3-1**). These results showed an effective blockage of γ-secretase activity and a consequent inhibition of Notch signaling by DAPT in the cultured tissues.

Next, we evaluate Notch signaling inhibition effects in the early-development of the thymus and parathyroid glands by measuring in the cultured pharyngeal explants the expression of *Foxn1* and *Gcm2*, respectively.

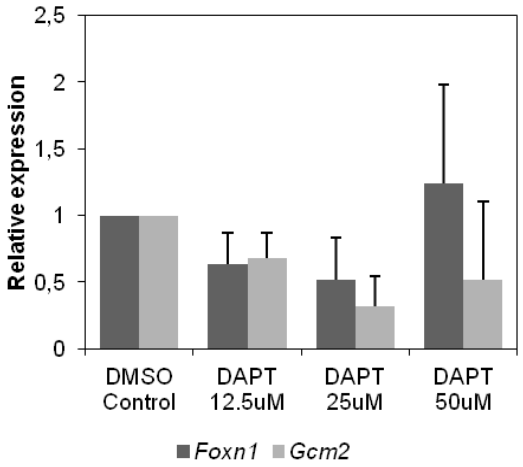


**Figure 3-3** Relative expression of *Foxn1* and *Gcm2* in the pharyngeal region explants grown with increasing concentrations of DAPT. 5 samples for each culture conditions.

**Table 3-2** *Foxn1* **(A)** and *Gcm2* **(B)** expression in the pharyngeal region explants.

**A**

| *Foxn1* | Average | StDev | p-value |
|---|---|---|---|
| DMSO Control | 1,000 | - | - |
| DAPT 12.5μM | 0,635 | 0,236 | 0,085 |
| DAPT 25μM | 0,517 | 0,315 | 0,192 |
| DAPT 50μM | 1,243 | 0,735 | 0,760 |

**B**

| *Gcm2* | Average | StDev | p-value |
|---|---|---|---|
| DMSO Control | 1,000 | - | - |
| DAPT 12.5μM | 0,676 | 0,194 | 0,219 |
| DAPT 25μM | 0,318 | 0,224 | 0,172 |
| DAPT 50μM | 0,513 | 0,593 | 0,258 |

In **Figure 3-3**, explants treated with increasing doses of DAPT (all concentrations) showed lower *Foxn1 and Gcm2* expression when compared with control conditions, with the exception of *Foxn1* expression in 50μM DAPT-explants (which showed similar levels to control) (**Table 3-2**).

3.1.2 LY411575:

Similar experimental approach was performed to study Notch inhibition effects using LY411575 inhibitor.

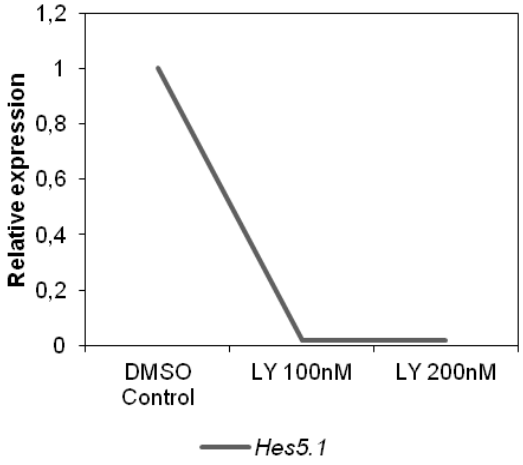


**Table 3-3** *Hes5.1* expression in the pharyngeal region explants

| *Hes5.1* | Average | StDev | p-value |
|---|---|---|---|
| DMSO Control | 1,000 | - | - |
| LY 100nM | 0,019 | 0,016 | 0,103 |
| LY 200nM | 0,017 | 0,012 | 0,051 |

**Figure 3-4** Relative expression of *Hes5.1* in the pharyngeal region explants grown at increased concentrations of LY411575 (LY). 5 samples for each culture conditions.

When pharyngeal explants were grown in the presence of 100nM (0.1% DMSO) and 200nM (0.2% DMSO) of LY411575 we observed an effective decrease of *Hes5.1* expression when compared to the control explants (**Figure 3-4** and **Table 3-3**). The results obtained with

LY411575, were similar to those obtained with DAPT, which showed an effective Notch signaling inhibition when using these inhibitors. However, in this case, Notch inhibition was not dose-dependent.

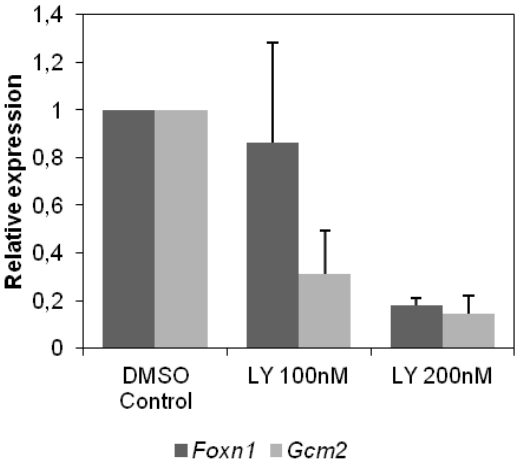


**Figure 3-5** Relative expression of *Foxn1* and *Gcm2* in the pharyngeal region explants grown with increasing concentrations of LY411575 (LY). 5 samples for each culture conditions.

**Table 3-4** *Foxn1* **(A)** and *Gcm2* **(B)** expression in the pharyngeal region explants.

**A**

| *Foxn1* | Average | StDev | p-value |
|---|---|---|---|
| DMSO Control | 1,000 | - | - |
| LY 100nM | 0,861 | 0,422 | 0,697 |
| LY 200nM | 0,182 | 0,030 | 0,034 |

**B**

| *Gcm2* | Average | StDev | p-value |
|---|---|---|---|
| DMSO Control | 1,000 | - | - |
| LY 100nM | 0,310 | 0,182 | 0,166 |
| LY 200nM | 0,146 | 0,074 | 0,112 |

The effect of Notch signaling inhibition in the early-development of the glands was measured in the cultured pharyngeal explants by evaluating the expression of *Foxn1* and *Gcm2*, respectively. As reported in DAPT-explants, a reduction of *Foxn1* and *Gcm2* expression was observed in explants treated with increasing doses of LY411575 inhibitor (100nM and 200nM) when compared to control conditions (**Figure 3-5** and **Table 3-4**).

## 3.2. Pharmacological inhibition of Notch signaling in heterospecific association of tissues

To study Notch signaling effects during cellular interactions between the 3/4 PP endoderm and the ectopic/permissive mesenchyme (somatopleura), heterospecific associations of these tissues were grown in the presence of 50µM of DAPT, as described above. After 48h of culture, Notch signaling inhibition was evaluated by the expression of Notch target gene *Hes5.1*, and its effects in thymus and parathyroid glands organogenesis by *Foxn1* and *Gcm2* expression, respectively. Gene expression was quantified using Quantitative Real-Time PCR analysis.

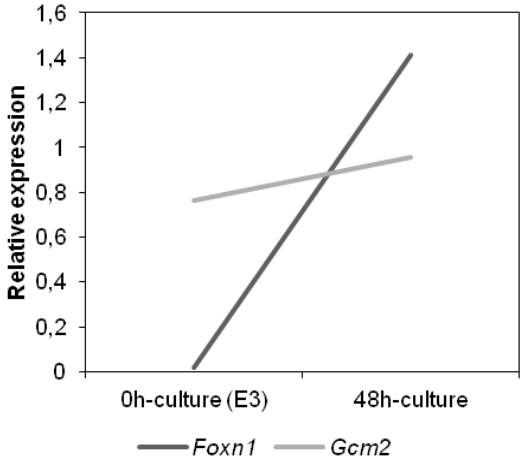


**Figure 3-6** Relative expression of *Foxn1*, *Gcm2* and *Hes5.1* in freshly isolated quail 3/4 PP endoderm (E3) and after 48h of culture in control culture medium (RPMI-1640 supplemented with 10% FBS, 1x Pen/Strep). 0h-culture, n=3; 48h-culture, n=2.

We started to measure the initial expression of *Foxn1* and *Gcm2* in freshly isolated 3/4 PP endoderm and then after 48h of culture in heterospecific associations. As depicted in **Figure 3-6**, we observed almost no expression of *Foxn1* at the beginning of the culture, while *Gcm2* had already moderate levels of expression. After the 48h of culture, a striking increase of *Foxn1* expression was observed accompanied by maintenance of *Gcm2* expression.

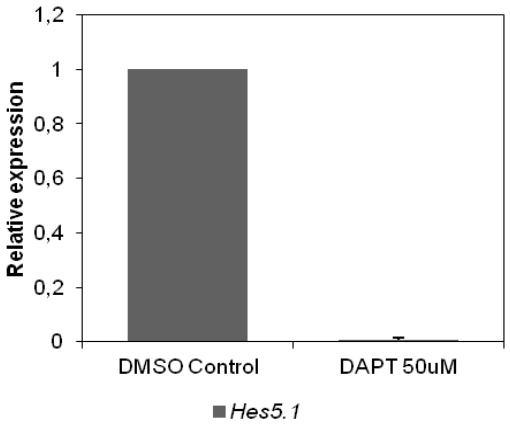


**Table 3-5** *Hes5.1* expression in the heterospecific association of tissues.

| *Hes5.1* | Average | StDev | p-value |
|---|---|---|---|
| DMSO Control | **1,000** | **-** | **-** |
| DAPT 50μM | **0,008** | **0,008** | **0,418** |

**Figure 3-7** Relative expression of *Hes5.1* in heterospecific association of tissues grown in the presence of 50μM DAPT. 3 samples for each culture conditions.

As shown in **Figure 3-7**, when the associated tissues were grown for 48h in the presence of 50μM DAPT we observed a decrease of 99,2% in *Hes5.1* expression, showing the inhibition of Notch signaling by the blockage of γ-secretase activity. We then measured the Notch signaling inhibition effect in the levels of expression of *Foxn1* and *Gcm2*.

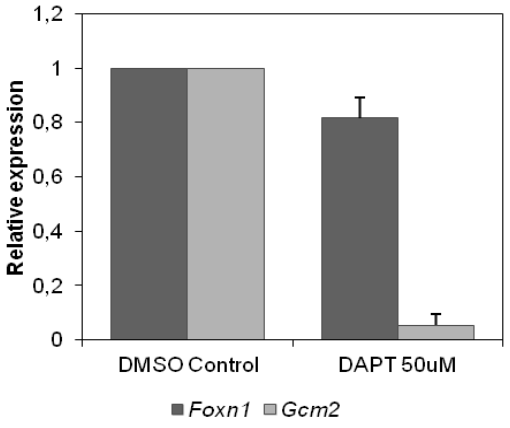


**Figure 3-8** Relative expression of *Foxn1* and *Gcm2* in the heterospecific association tissues grown in the presence of 50μM DAPT. 3 samples for each culture conditions.

**Table 3-6** *Foxn1* **(A)** and *Gcm2* **(B)** expression in the heterospecific association of tissues.

**A**

| *Foxn1* | Average | StDev | p-value |
|---|---|---|---|
| DMSO Control | 1,000 | - | - |
| DAPT 50μM | 0,817 | 0,074 | 0,454 |

**B**

| *Gcm2* | Average | StDev | p-value |
|---|---|---|---|
| DMSO Control | 1,000 | - | - |
| DAPT 50μM | 0,055 | 0,040 | 0,070 |

Similar to 50μM DAPT-explants, *Gcm2* expression was reduced in the associated tissues grown in the presence of DAPT (**Figure 3-8** and **Table 3-6**). However, the expression of *Foxn1* in the associated tissues was lower than the control and distinct to what was observed in the pharyngeal explants experiments.

## 3.3. Modulation of Notch signaling in the prospective domains of the thymus and parathyroid glands (3/4 PP endoderm)

### 3.3.1 Production of pT2K-NLS-Cherry-DNMAML1

In a distinct approach, we aimed to modify Notch signaling in the prospective domain of thymus and parathyroid glands. Gain- and loss- of function experiments were performed using two recombinant plasmids containing either the intracellular domain of Notch1 (ICN1) or the dominant-negative form of MAML1 (DNMAML1), respectively. *ICN1* or *DNMAML1* sequences were previously cloned into pT2K-BI-TREeGFP thus generating pT2K-ICN1eGFP and pT2K-DNMAML1eGFP (Figueiredo, 2011). As *DNMAML1* sequence is only 200bp, generating a small protein that might be unstable, we generated a new construct adding to the *DNMAML1* sequence a *CherryNLS* (Cherry Nuclear Localization Sequence) with 761bp. With this approach, we hope to generate a more stable DNMAML1 protein, more competitive against endogenous MAML1. *DNMAML1* sequence in fusion with *CherryNLS* sequence was cloned in pT2K-BI-TREeGFP, generating pT2K-NLS-Cherry-DNMAML1eGFP plasmid.

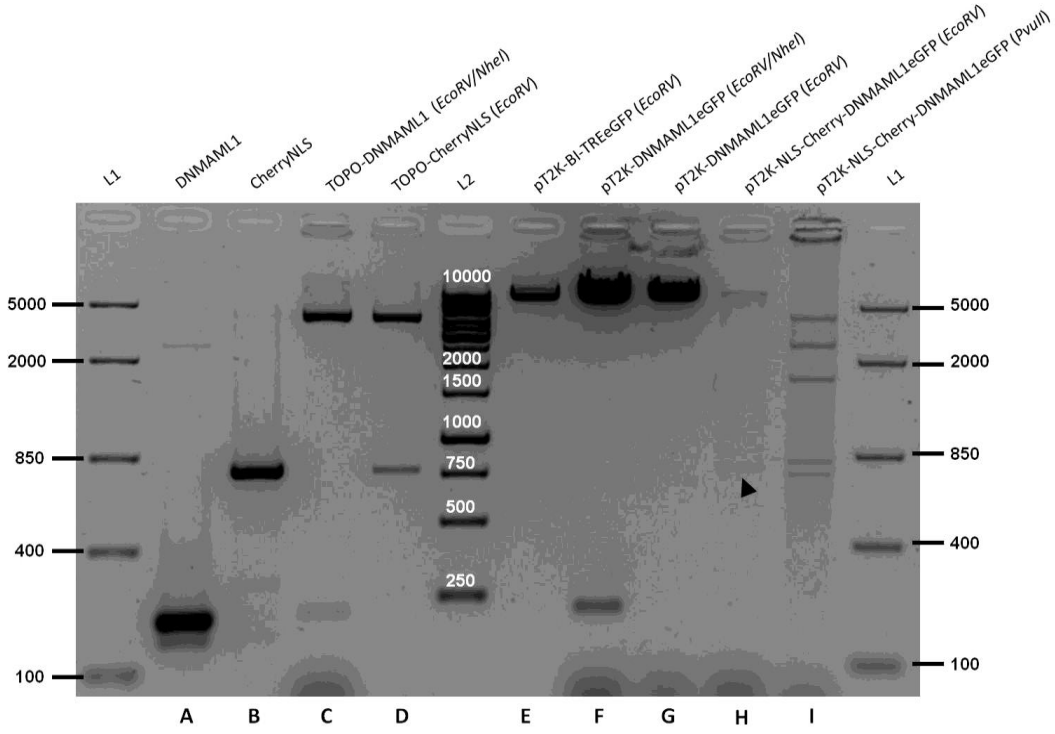


**Figure 3-9 1.3% Agarose gel electrophoresis showing the steps involved on the generation of pT2K-NLS-Cherry-DNMAML1eGFP.** PCR amplification of *DNMAML1* (A). PCR amplification of *CherryNLS* (B). TOPO-DNMAML1 digested with *EcoRV/NheI* (C). TOPO-CherryNLS digested with *EcoRV* (D). pT2K-BI-TREeGFP linearized with *EcoRV* (E). pT2K-DNMAML1eGFP digested with *EcoRV/NheI* (F). pT2K-DNMAML1eGFP linearized with *EcoRV* (G). pT2K-NLS-Cherry-DNMAML1eGFP digested with *EcoRV* (H). Confirmation of *CherryNLS* insert orientation on the final plasmid by digestion with *PvuII* (I). L1, O'GeneRuler™ 1 kb DNA Ladder; L2, FastRuler™ Middle Range DNA Ladder. Arrowhead indicates the DNA band corresponding to the *CherryNLS* sequence in pT2K-NLS-Cherry-DNMAML1eGFP.

The first step for the production of pT2K-NLS-Cherry-DNMAML1 was the PCR amplification of *DNMAML1* (205bp) from a cE3 embryo cDNA (**Figure 3-9 A**), and

*CherryNLS* (761bp) from a pCAG plasmid (pCAG-CherryNLS; Vilas-Boas, 2011) (**Figure 3-9 B**). Each PCR product was cloned in a pCR®II-TOPO® vector (4kb). According to the inserted restriction sites, the presence of *DNMAML1* in TOPO-DNMAML1 was confirmed by double digestion with *EcoRV* and *NheI*, and single digestion with *EcoRV* for the presence of *CherryNLS* in TOPO-CherryNLS. As expected and shown in **Figure 3-9** (**C** and **D**), there are two bands in each case: a 4kb DNA band corresponding to the pCR®II-TOPO® vector and a 205bp DNA band for *DNMAML1* or 761bp DNA band for *CherryNLS* fragments.

Secondly, the *EcoRV/NheI DNMAML1* insert was purified from TOPO-DNMAML1 and subcloned into the pT2K-BI-TREeGFP plasmid (8,7Kb). The presence of *DNMAML1* insert was confirmed as described earlier, and two bands were obtained: an 8.7Kb and a 205bp DNA fragments corresponding to pT2K-BI-TREeGFP plasmid and *DNMAML1* insert, respectively (**Figure 3-9 F**). The integrity of pT2K-BI-TREeGFP plasmid was ensured by the presence of an 8.7kb DNA band when linearized with *EcoRV* (**Figure 3-9 E**).

Once generated pT2K-DNMAML1eGFP, the *CherryNLS* sequence was cloned in fusion to DNMAML1. For that, the *EcoRV CherryNLS* sequence was purified from TOPO-CherryNLS and subcloned in the previous recombinant plasmid pT2K-DNMAML1eGFP (digested with *EcoRV* and dephosphorylated) (**Figure 3-9 G**), thus generating pT2K-NLS-Cherry-DNMAML1eGFP. The single digestion with *EcoRV* confirmed the presence of a 761bp DNA band corresponding to the *CherryNLS* sequence (**Figure 3-9 H**, arrowhead). Finally, the correct orientation of the insert was confirmed by single digestion of the final plasmid pT2K-NLS-Cherry-DNMAML1eGFP with *PvuII*, giving rise to five expected DNA fragments (2513bp + 746bp + 1711bp + 793bp + 3904bp) (**Figure 3-9 I**).

### 3.3.2 Establishment of electroporation of the 3/4 PP endoderm conditions

To modulate Notch signaling in the prospective domains of the thymus and parathyroid glands, the 3/4 PP endoderm was genetically modified using a combined system of vectors: *Tol2*-mediated gene transfer technique and Tetracycline-dependent conditional gene expression (Sato et al., 2007; Watanabe et al., 2007). First, the isolated quail 3/4 PP endoderm was electroporated with distinct vectors: pT2K-BI-TREeGFP (control condition); pT2K-ICN1eGFP (gain-of-function condition); pT2K-DNMAML1eGFP (1$^{st}$ loss-of-function condition); and pT2K-NLS-Cherry-DNMAML1eGFP (2$^{nd}$ loss-of function condition). For each condition, the vector was co-electroporated with pT2K-CAGGS-tTA (transactivator), which modulates the expression of the first. Genetically modified endoderm was then associated with chicken mesenchyme and allowed to grow for 48h. Quantitative gene expression analysis was performed to the cultured tissues for *Hes5.1* (Notch target), *Foxn1* (thymic epithelial marker), *Gcm2* (parathyroid epithelial marker) and *GFP* (vector marker) genes. However, and in contrast with the previous experiments, *Hes5.1* expression could not be

measured as a direct readout of Notch signaling inhibition (in the endoderm), as the mesenchymal compartment of the heterospecific association of tissues could also express *Hes5.1*. The vector-specific expression of Intracellular domain of Notch 1 (ICN1) and Dominant Negative form of Mastermind-like 1 (DNMAML1) was also evaluated by qRT-PCR in the respective culture conditions.

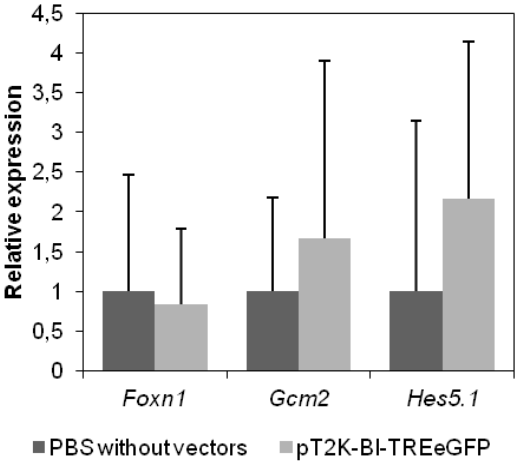


**Figure 3-10** Relative expression of *Foxn1*, *Gcm2* and *Hes5.1* in the heterospecific association of tissues after 48h of culture. Two control conditions of electroporation were evaluated: endoderm electroporated with PBS without vectors and with the control vector, the pT2K-BI-TREeGFP. PBS w/o vectors, n=5; pT2K-BI-TREeGFP, n=3.

**Table 3-7** *Foxn1* **(A)**, *Gcm2* **(B)** and *Hes5.*1 **(C)** expression in the heterospecific association of tissues.

**A**

| *Foxn1* | Average | StDev | p-value |
|---|---|---|---|
| PBS w/o vectors | 1,000 | 1,463 | - |
| pT2K-BI-TREeGFP | 0,843 | 0,939 | 0,860 |

**B**

| *Gcm2* | Average | StDev | p-value |
|---|---|---|---|
| PBS w/o vectors | 1,000 | 1,181 | - |
| pT2K-BI-TREeGFP | 1,671 | 2,227 | 0,666 |

**C**

| *Hes5.1* | Average | StDev | p-value |
|---|---|---|---|
| PBS w/o vectors | 1,000 | 2,151 | - |
| pT2K-BI-TREeGFP | 2,169 | 1,977 | 0,471 |

To assess the endodermal effects of the electroporation with the system of vectors, we used two distinct control conditions of electroporation: PBS without vectors and the control vector, the pT2K-BI-TREeGFP. No significant differences were observed for *Foxn1*, *Gcm2* and *Hes5.1* expression in the two conditions (**Figure 3-10** and **Table 3-7**). However, a tendency for increased expression of *Gcm2* and *Hes5.1* was observed when the endoderm was electroporated with pT2K-BI-TREeGFP. Thus, samples electroporated with the control vector were used as the calibrator for the following experiments.

### 3.3.3 Loss-of-function of Notch signaling by genetic modification of the 3/4PP endoderm

Loss-of-function experiments were performed using two distinct constructs: pT2K-DNMAML1eGFP and pT2K-NLS-Cherry-DNMAML1eGFP. DNMAML1 is a dominant-negative form of the co-activator MAML1 that competes with its native form for the binding of ICN, and blocks the activity of Notch signaling.

Endoderm was electroporated with either control or loss-of-function vectors. After 48h of culture with the mesenchyme, the associated tissues were collected and analysed for *GFP* and *DNMAML1* (construct) expression.

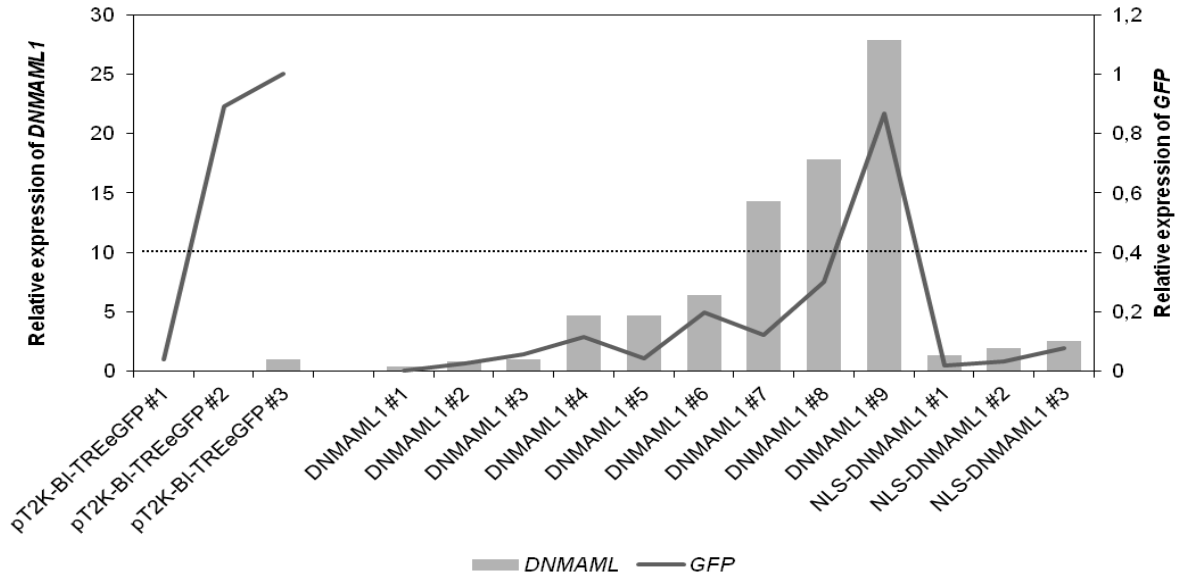


**Figure 3-11** Expression of *DNMAML1* and *GFP* in the heterospecific association of tissues after 48h of culture. Endoderm was electroporated with the control vector (pT2K-BI-TREeGFP), pT2K-DNMAML1eGFP (DNMAML1 samples) or pT2K-NLS-Cherry-DNMAML1eGFP (NLS-DNMAML1 samples).

As shown in **Figure 3-11**, the expression of *GFP* and *DNMAML1* was widely variable among the different samples of the associated tissues. Moreover, we observed a strong correlation with the levels of expression of *GFP* and *DNMAML1*. Samples were divided in three distinct groups: low (<3), medium (3-10), or high (>10) *DNMAML1* (*GFP*) expression. According to this criterion, the expression of *DNMAML1* observed for the new construct, the pT2K-NLS-Cherry-DNMAML1eGFP, was considered to be low (<3). The expression of *Foxn1*, *Gcm2* and *Hes5.1* was further evaluated in each of these sample groups.

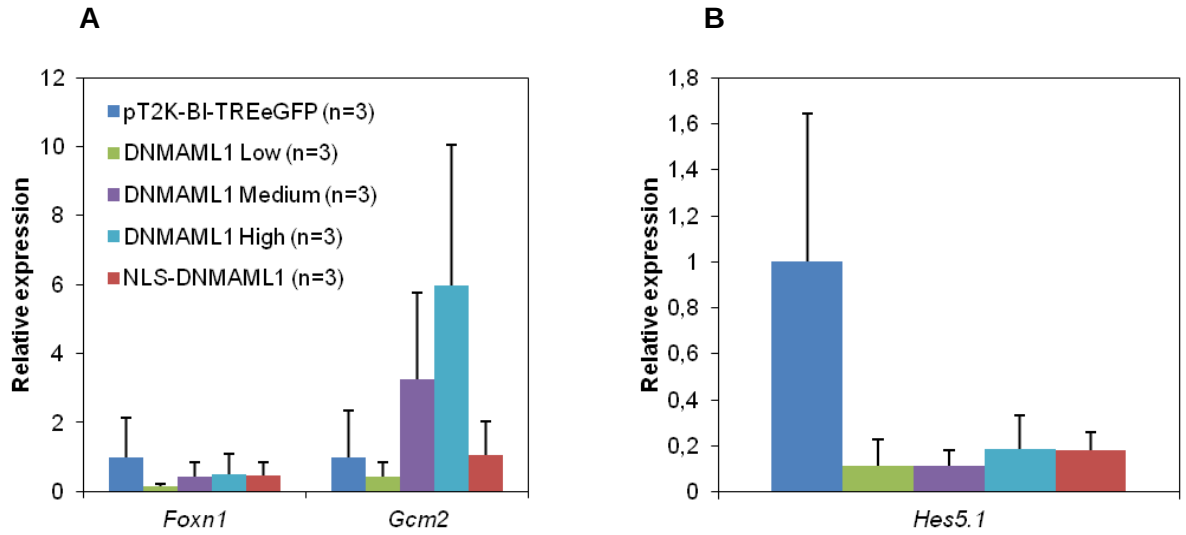


**Figure 3-12** Relative expression of *Foxn1*, *Gcm2* **(A)** and Hes5.1 **(B)** of the heterospecific association of tissues grown for 48h in culture. Endoderm was electroporated with the control vector (pT2K-BI-TREeGFP), pT2K-DNMAML1eGFP or pT2K-NLS-Cherry-DNMAML1eGFP.

As shown in **Figure 3-12** and **Table 6-3**, a reduction of *Foxn1* expression was observed in the endoderm electroporated with the loss-of-function vectors independently of the levels of the construct expression, when compared to control conditions. *Gcm2* showed an increased expression in the conditions with the highest levels of *DNMAML1* construct expression. Finally, *Hes5.1* was reduced in all samples electroporated with loss-of-function vectors when compared with control condition. However, *Hes5.1* expression is a combined readout of its expression in the endodermal and mesenchymal compartments of the associated tissues, not reflecting the Notch signaling activity in the modified endoderm.

### 3.3.4 Gain-of-function of Notch signaling by genetic modification of the 3/4PP endoderm

Gain-of-function experiments were performed by electroporating 3/4 PP endoderm with the construct pT2K-ICN1eGFP. The expression of the intracellular domain of Notch 1 (ICN1) constitutively activates Notch signaling in a ligand-independent manner. Similar to DNMAML1 experiments, the expression of *GFP* and *ICN1* in each electroporated sample (control and gain-of-function vectors) was measured.

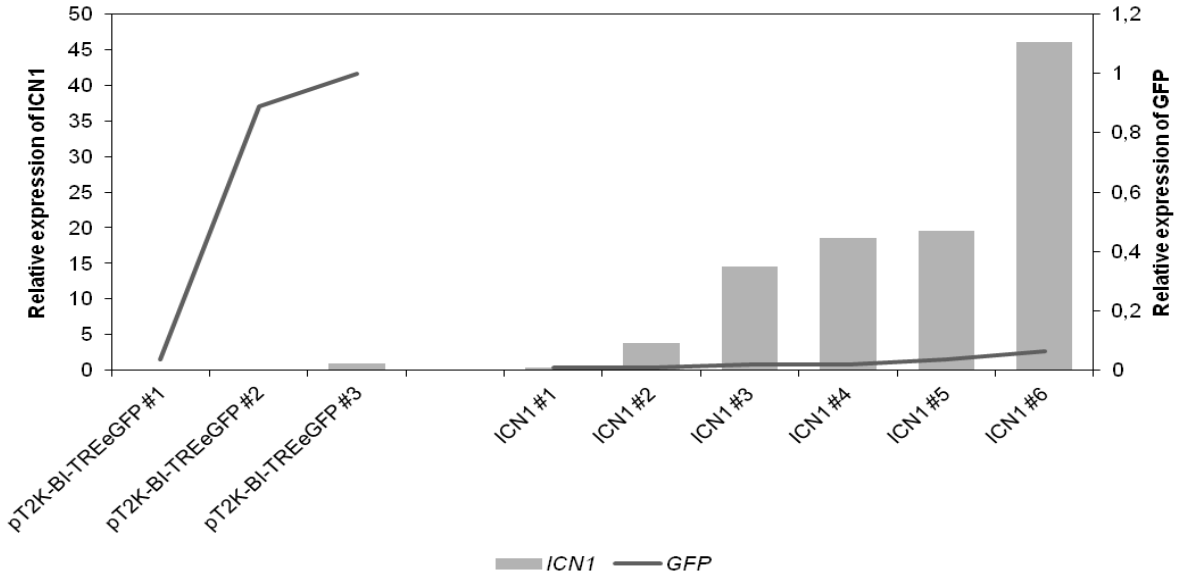


**Figure 3-13** Expression of *ICN1* and *GFP* in the heterospecific association of tissues after 48h of culture. Endoderm was electroporated with the control vector (pT2K-BI-TREeGFP) or pT2K-ICN1eGFP (ICN1 samples).

As shown in **Figure 3-13**, the expression of *GFP* and *ICN1* was also widely variable among the different samples, such as seen for *DNMAML1*. However, for similar construct expression level, the expression of *GFP* was lower in ICN1 samples when compared to its expression in *DNMAML1* samples. Samples were divided in two distinct groups: low/medium (<10) or high (≥10) ICN1 expression. The expression of *Foxn1*, *Gcm2* and *Hes5.1* was further evaluated in each of these sample groups.

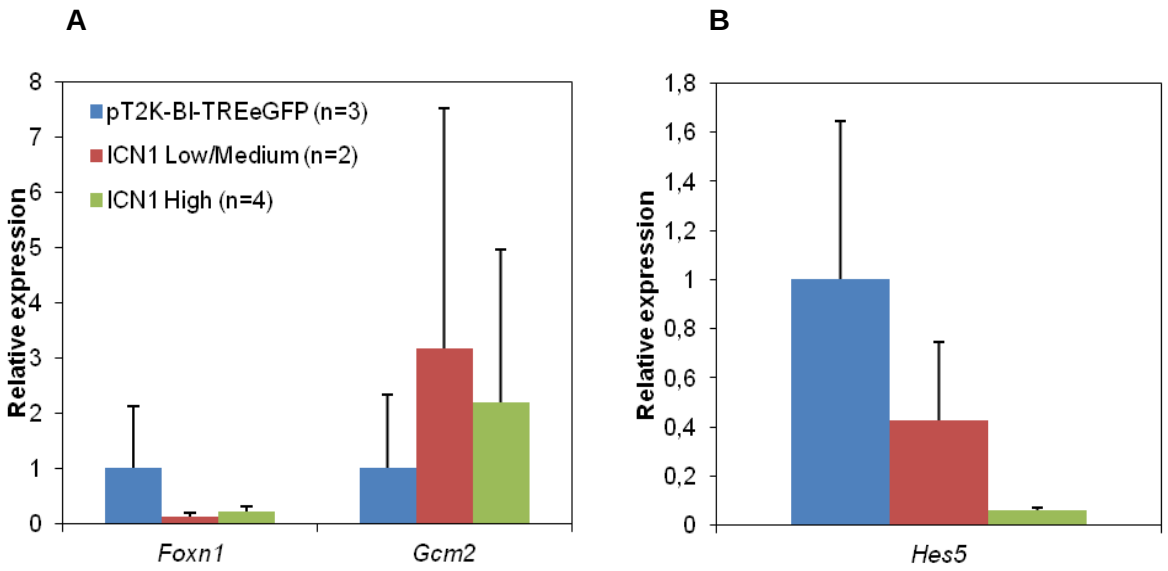


**Figure 3-14** Relative expression of *Foxn1*, *Gcm2* **(A)** and *Hes5.1* **(B)** of the heterospecific association of tissues grown for 48h in culture. Endoderm was electroporated with the control vector (pT2K-BI-TREeGFP) or pT2K-ICN1eGFP.

As shown in **Figure 3-14** and **Table 6-4**, a reduction of *Foxn1* and an increase of Gcm2 expression was observed in the endoderm electroporated with the gain-of-function vector (independently of the levels of the construct expression), when compared to control conditions. Surprisingly, *Hes5.1* was also reduced in all samples electroporated with ICN vector when compared with control condition.

## 4. DISCUSSION

The aim of this project was to unravel the role of Notch signaling during the early stages of the avian thymus and parathyroid glands organogenesis. The manipulation of Notch signaling was achieved *in vitro* by two distinct approaches: pharmacological inhibition and gain- or loss-of-function of Notch signaling by genetic manipulation of the prospective territories of the thymus and parathyroid glands. Analysis of the effects of Notch signaling modulation was performed by measuring the expression by quantitative RT-PCR of the transcription factors, *Hes5.1* (Notch-target gene), *Foxn1* (marker for thymus epithelium) and *Gcm2* (marker for parathyroid glands epithelium) in the distinct samples.

The pharmacological inhibition of Notch signaling promoted a decrease of *Foxn1* (with only one exception) and *Gcm2* expression. These results suggest that blocking Notch signaling in the endodermal and mesenchymal compartment impairs normal development of these glands.

When Notch signaling was modulated in the developing 3/4 PP endoderm to constitutively express ICN1 (gain-of-function) or DNMAML1 (loss-of-function) constructs we observed a

reduction of *Foxn1* expression accompanied by an increase of *Gcm2*. This conflicting data will be subject to further discussion bellow.

### 4.1. *In vitro* development of the thymic and parathyroid rudiments (3/4 PP endoderm)

In this work we used two distinct organotypic systems of culture to mimic early development of the thymus and parathyroid glands. In the first, the pharyngeal region of E3 quail embryos was isolated and grown *in vitro* for 48h. In the second, isolated quail endoderm of 3/4PP (E3) and isolated chick mesenchyme of the somatopleura (E2.5) were associated *in vitro* for 48h. This system was previously used and validated to its capacity to reproduce early events in the development of these glands by our group (Neves et al., 2012). In this work, variation of levels of expression of *Foxn1* and *Gcm2* throughout the time of culture was similar to those previously reported (Neves et al., 2012).

In the pharyngeal explants culture, as opposed to observed in the association tissue system of culture, we observed a slight reduction of *Gcm2* expression after 48h of culture. For this unexpected result we cannot exclude some effects resulting from 3D-constrains to nutrients and oxygen accessibility in this type of culture system. However, *Hes5.1* showed a strong increased expression in the explant samples. In agreement, we have previously observed this augmentation of *Hes5.1* expression, by whole-mount (WM) in situ hybridization, in chick E3.5 (corresponding to quail E3) explants grown in similar conditions (Figueiredo, 2011).

Furthermore, we recently observed strong expression of Notch-related genes (receptors, ligands and target-genes) in the endoderm of the 3/4 PP and surrounding mesenchyme by WM in situ hybridization and microarray techniques (data not shown of recent studies from our team).

Together, these results strongly suggest that Notch signaling is active during these early events of thymic and parathyroid glands organogenesis.

### 4.2. Pharmacological inhibition of Notch signaling impairs early-development of thymus and parathyroid glands.

In this work, we started to manipulate Notch signaling by a γ-secretase inhibitor, DAPT, in both of our culture systems. We observed a decrease of *Foxn1* (with only one exception) and *Gcm2* expression in the endoderm grown in its 3D-preserved environment (pharyngeal explants) or when associated with an ectopic mesenchyme (somatopleural mesenchyme). These results suggest that inhibition of Notch signal in the epithelial and mesenchymal compartments may interfere with normal establishing of thymus and parathyroid glands rudiments. Moreover, it also shows similar Notch effects when the endoderm interacts with the natural or the ectopic mesenchymal tissues.

Only when pharyngeal explants were grown in the presence of 50μM DAPT, we observed a slight increase in *Foxn1* expression. Though unexpected, similar results were obtained from our group in previous studies (Figueiredo, 2011). Chicken pharyngeal explants of E3.5 (corresponding to quail E3) grown in similar conditions and WM in situ hybridized showed a complete abrogation of *Gcm2* signals while *Foxn1* was randomly expressed.

To validate Notch signaling effects by the inhibition of DAPT we pursued our studies using another Notch inhibitor, LY411575. Similar results were obtained with pharyngeal explants grown in the presence of LY411575 when compared with those grown with DAPT. In fact, a more pronounced effect was observed in Ly411575-explants. We are now evaluating the effect of this inhibitor in the culture of heterospecific association of tissues.

The interaction between Notch signals and *Foxn1* and *Gcm2* expression has been described in other developmental contexts. In fact, a mutual regulation of Notch signaling and *Foxn1* during hair follicle differentiation has been shown (Hu et al., 2010, Cai et al., 2009), as well as a role for *Gcm2* in the expression of *Hes5* during the generation of neural stem cells (Hitoshi et al., 2011).

Taken together, our results show a tendency for a reduction of *Foxn1* and *Gcm2* expression (although not significant), in all condition where Notch signaling is inhibited. These suggest that the pharmacological inhibition of Notch impairs the normal organogenesis of the thymus and parathyroid glands.

### 4.3. Genetic modification of the prospective domains of the thymus and parathyroid glands (3/4 PP endoderm) with gain-and loss-of-function of Notch

To modulate Notch signaling exclusively in the prospective domains of the thymus and parathyroid glands, we genetically modified the 3/4 PP endoderm using a system of vectors combining a *Tol2*-mediated gene transfer technique and a Tetracycline-dependent conditional gene expression. To manipulate Notch signaling, three constructs were used: pT2K-ICN1eGFP (ICN1, gain-of-function), pT2K-DNMAML1eGFP (DNMAML1, loss-of-function) [both developed in a previous work (Figueiredo, 2011)] and a new construct developed in this work, the pT2K-NLS-Cherry-DNMAML1eGFP (NLS-DNMAML1), carrying a more stable and efficient form of DNMAML1.

To evaluate the loss-of-function of Notch in the prospective domains of the glands, the isolated 3/4 PP endoderm was genetically modified with the constructs (DNMAML1 or NLS-DNMAML1) and grown for 48h in heterospecific association with non-modified ectopic mesenchyme. We observed a slight reduction of *Foxn1* and *Gcm2* expression when low levels of the construct were observed. This is in agreement with our results obtained when Notch signaling was pharmacologically inhibited. However, samples with medium/high doses of the DNMAML1 construct showed an up-regulation of *Gcm2* expression. This distinct effect

in *Gcm2* expression may be dose-dependent and/or due to the different cellular interactions responses between the manipulated endoderm with different levels of Notch signal and the non-manipulated mesenchyme. We may further envisage a cell-autonomous effect of Notch signaling reduction (block) to promote parathyroid glands development. Though intriguing, the results obtained cannot be explained by the non-functional constructs as they were previously tested in vivo (data not shown from our team). The loss-of-function constructs (DNMAML1 or NLS-DNMAML1) were *in ovo* electroporated in the neural tube and the expected *Hes5.1* reduction was observed (Vilas-Boas et al., 2011), confirming the constructs functionality.

Finally, we evaluated the gain-of-function of Notch in the prospective domains of the glands by genetically modifying the endoderm with the ICN1 construct. Unexpectedly and similar to observed in the loss-of-function assays, when the endoderm was manipulated to over express ICN1 we observed a reduction of *Foxn1* and an increase of *Gcm2* expression. We are now conducting new experiments to evaluate the functionality of the ICN1 construct as its incapacity to activate Notch signaling may explain the results obtained.

## 5. REFERENCES


**Alcobia, I., Gomes, A., Saavedra, P., Laranjeiro, R., Oliveira, S., Parreira, L. and Cidadão, A.** (2011). Portrayal of the Notch system in embryonic stem cell-derived embryoid bodies. *Cells, tissues, organs* **193**, 239–52.

**Alves, N. L., Huntington, N. D., Rodewald, H.-R. and Di Santo, J. P.** (2009). Thymic epithelial cells: the multi-tasking framework of the T cell “cradle”. *Trends in immunology* **30**, 468–74.

**Anderson, G. and Jenkinson, E. J.** (2001). Lymphostromal interactions in thymic development and function. *Nature reviews. Immunology* **1**, 31–40.

**Blackburn, C. C. and Manley, N. R.** (2004). Developing a new paradigm for thymus organogenesis. *Nature reviews. Immunology* **4**, 278–89.

**Blackburn, C. C., Augustine, C. L., Li, R., Harvey, R. P., Malin, M. a, Boyd, R. L., Miller, J. F. and Morahan, G.** (1996). The nu gene acts cell-autonomously and is required for differentiation of thymic epithelial progenitors. *Proceedings of the National Academy of Sciences of the United States of America* **93**, 5742–6.

**Bockman, D. and Kirby, M.** (1984). Dependence of thymus development on derivatives of the neural crest. *Science (New York, NY)* **223**, 498–500.

**Bray, S. J.** (2006). Notch signalling: a simple pathway becomes complex. *Nature reviews. Molecular cell biology* **7**, 678–89.

**Cai, J., Lee, J., Kopan, R. and Ma, L.** (2009). Genetic interplays between *Msx2* and *Foxn1* are required for Notch1 expression and hair shaft differentiation. *Developmental biology* **326**, 420–430.

**Candi, E., Rufini, A., Terrinoni, A., Giamboi-Miraglia, A., Lena, A. M., Mantovani, R., Knight, R. and Melino, G.** (2007). DeltaNp63 regulates thymic development through enhanced expression of *FgfR2* and *Jag2*. *Proceedings of the National Academy of Sciences of the United States of America* **104**, 11999–2004.

**Conlon, R. a, Reaume, a G. and Rossant, J.** (1995). Notch1 is required for the coordinate segmentation of somites. *Development (Cambridge, England)* **121**, 1533–45.

**Dorshkind, K., Montecino-Rodriguez, E. and Signer, R. a J.** (2009). The ageing immune system: is it ever too old to become young again? *Nature reviews. Immunology* **9**, 57–62.

**Douarin, N. Le and Jotereau, F.** (1975). Tracing of cells of the avian thymus through embryonic life in interspecific chimeras. *The Journal of experimental medicine* **142**,.

**Dovey, H. F., John, V., Anderson, J. P., Chen, L. Z., De Saint Andrieu, P., Fang, L. Y., Freedman, S. B., Folmer, B., Goldbach, E., Holsztynska, E. J., et al.** (2001). Functional gamma-secretase inhibitors reduce beta-amyloid peptide levels in brain. *Journal of neurochemistry* **76**, 173–81.

**Farley, A. M., Morris, L. X., Vroegindeweij, E., Depreter, M. L. G., Vaidya, H., Stenhouse, F. H., Tomlinson, S. R., Anderson, R. a, Cupedo, T., Cornelissen, J. J., et al.** (2013). Dynamics of thymus organogenesis and colonization in early human development. *Development (Cambridge, England)* **140**, 2015–26.

**Fauq, A. H., Simpson, K., Maharvi, G. M., Golde, T. and Das, P.** (2007). A multigram chemical synthesis of the g-secretase inhibitor LY411575 and its diastereoisomers. **17**, 6392–6395.

**Figueiredo, M.** (2011). The role of Notch signaling in thymic epithelium development. *Master's thesis, Universidade de Lisboa.*

**Fiorini, E., Merck, E., Wilson, A., Ferrero, I., Jiang, W., Koch, U., Auderset, F., Laurenti, E., Tacchini-Cottier, F., Pierres, M., et al.** (2009). Dynamic regulation of *notch* 1 and *notch* 2 surface expression during T cell development and activation revealed by novel monoclonal antibodies. *Journal of immunology (Baltimore, Md. : 1950)* **183**, 7212–22.

**Fontaine-Perus, J. C., Calman, F. M., Kaplan, C. and Le Douarin, N. M.** (1981). Seeding of the 10-day mouse embryo thymic rudiment by lymphocyte precursors in vitro. *Journal of immunology (Baltimore, Md. : 1950)* **126**, 2310–6.

**Ge, Q. and Zhao, Y.** (2013). Evolution of thymus organogenesis. *Developmental and comparative immunology* **39**, 85–90.

**Gilmour, J.** (1939). The normal histology of the parathyroid glands. *The Journal of Pathology and Bacteriology*.

**Gordon, J. and Manley, N. R.** (2011). Mechanisms of thymus organogenesis and morphogenesis. *Development (Cambridge, England)* **138**, 3865–78.

**Gordon, J., Bennett, a R., Blackburn, C. C. and Manley, N. R.** (2001). *Gcm2* and *Foxn1* mark early parathyroid- and thymus-specific domains in the developing third pharyngeal pouch. *Mechanisms of development* **103**, 141–3.

**Graham, A. and Richardson, J.** (2012). Developmental and evolutionary origins of the pharyngeal apparatus. *EvoDevo* **3**, 24.

**Greenwald, I. and Kovall, R.** (2013). Notch signaling: genetics and structure. *WormBook : the online review of C. elegans biology* 1–28.

**Grevellec, A. and Tucker, A. S.** (2010). The pharyngeal pouches and clefts: Development, evolution, structure and derivatives. *Seminars in cell & developmental biology* **21**, 325–32.

**Griffith, A. V, Cardenas, K., Carter, C., Gordon, J., Iberg, A., Engleka, K., Epstein, J. a, Manley, N. R. and Richie, E. R.** (2009). Increased thymus- and decreased parathyroid-fated organ domains in Splotch mutant embryos. *Developmental biology* **327**, 216–27.

**Günther, T., Chen, Z. F., Kim, J., Priemel, M., Rueger, J. M., Amling, M., Moseley, J. M., Martin, T. J., Anderson, D. J. and Karsenty, G.** (2000). Genetic ablation of parathyroid glands reveals another source of parathyroid hormone. *Nature* **406**, 199–203.

**Hetzer-Egger, C., Schorpp, M., Haas-Assenbaum, A., Balling, R., Peters, H. and Boehm, T.** (2002). Thymopoiesis requires *Pax9* function in thymic epithelial cells. *European journal of immunology* **32**, 1175–81.

**Hitoshi, S., Alexson, T., Tropepe, V., Donoviel, D., Elia, A. J., Nye, J. S., Conlon, R. A., Mak, T. W., Bernstein, A. and Kooy, D. Van Der** (2002). Notch pathway molecules are essential for the maintenance , but not the generation , of mammalian neural stem cells. 846–858.

**Hitoshi, S., Ishino, Y., Kumar, A., Jasmine, S., Tanaka, K. F., Kondo, T., Kato, S., Hosoya, T., Hotta, Y. and Ikenaka, K.** (2011). Mammalian *Gcm* genes induce *Hes5* expression by active DNA demethylation and induce neural stem cells. *Nature Neuroscience* **14**, 957–964.

**Hu, B., Lefort, K. and Qiu, W.** (2010). Control of hair follicle cell fate by underlying mesenchyme through a CSL–Wnt5a–FoxN1 regulatory axis. *Genes & …* 1519–1532.

**Itoi, M., Kawamoto, H., Katsura, Y. and Amagai, T.** (2001). Two distinct steps of immigration of hematopoietic progenitors into the early thymus anlage. *International immunology* **13**, 1203–11.

**Jaleco, a C., Neves, H., Hooijberg, E., Gameiro, P., Clode, N., Haury, M., Henrique, D. and Parreira, L.** (2001). Differential effects of Notch ligands Delta-1 and Jagged-1 in human lymphoid differentiation. *The Journal of experimental medicine* **194**, 991–1002.

**Jiang, R., Lan, Y., Chapman, H. D., Shawber, C., Norton, C. R., Serreze, D. V., Weinmaster, G. and Gridley, T.** (1998). Defects in limb, craniofacial, and thymic development in *Jagged2* mutant mice. *Genes & Development* **12**, 1046–1057.

**Jiménez, E., Vicente, a, Sacedón, R., Muñoz, J. J., Weinmaster, G., Zapata, a G. and Varas, a** (2001). Distinct mechanisms contribute to generate and change the CD4:CD8 cell ratio during thymus development: a role for the Notch ligand, *Jagged1*. *Journal of immunology (Baltimore, Md. : 1950)* **166**, 5898–908.

**Kageyama, R., Ohtsuka, T. and Kobayashi, T.** (2007). The Hes gene family: repressors and oscillators that orchestrate embryogenesis. *Development (Cambridge, England)* **134**, 1243–51.

**Koch, Ute Fiorini, Emma Benedito, Rui Besseyrias, Valerie Schuster-Gossler, Karin Pierres, Michel Manley, Nancy R Duarte, Antonio Macdonald, H. R. R.** (2008). Delta-like 4 is the essential, nonredundant ligand for Notch1 during thymic T cell lineage commitment. *The Journal of experimental medicine* **205**, 2515–23.

**Kopan, R.** (2012). Notch signaling. *Cold Spring Harbor perspectives in biology* **4**,.

**Kopan, R. and Ilagan, M. X. G.** (2009). The canonical Notch signaling pathway: unfolding the activation mechanism. *Cell* **137**, 216–33.

**Koyanagi, A., Sekine, C. and Yagita, H.** (2012). Expression of Notch receptors and ligands on immature and mature T cells. *Biochemical and biophysical research communications* **418**, 799–805.

**Ladi, E., Yin, X., Chtanova, T. and Robey, E. a** (2006). Thymic microenvironments for T cell differentiation and selection. *Nature immunology* **7**, 338–43.

**Laranjeiro, R., Alcobia, I., Neves, H., Gomes, A. C., Saavedra, P., Carvalho, C. C., Duarte, A., Cidadão, A. and Parreira, L.** (2012). The notch ligand delta-like 4 regulates multiple stages of early hemato-vascular development. *PloS one* **7**, e34553.

**Le Douarin, N. M. and Teillet, M. a** (1973). The migration of neural crest cells to the wall of the digestive tract in avian embryo. *Journal of embryology and experimental morphology* **30**, 31–48.

**Lindsay, E. a** (2001). Chromosomal microdeletions: dissecting del22q11 syndrome. *Nature reviews. Genetics* **2**, 858–68.

**Liu, Z., Shirakawa, T., Li, Y., Soma, A., Oka, M., Dotto, G. P., Fairman, R. M., Velazquez, O. C. and Herlyn, M.** (2003). Regulation of *Notch1* and *Dll4* by Vascular Endothelial Growth Factor in Arterial Endothelial Cells : Implications for Modulating Arteriogenesis and Angiogenesis. **23**, 14–25.

**Liu, Z., Yu, S. and Manley, N. R.** (2007). *Gcm2* is required for the differentiation and survival of parathyroid precursor cells in the parathyroid/thymus primordia. *Developmental biology* **305**, 333–46.

**Livak, K. J. and Schmittgen, T. D.** (2001). Analysis of relative gene expression data using real-time quantitative PCR and the 2(-Delta Delta C(T)) Method. *Methods (San Diego, Calif.)* **25**, 402–8.

**Maillard, I., Weng, A. P., Carpenter, A. C., Rodriguez, C. G., Sai, H., Xu, L., Allman, D., Aster, J. C. and Pear, W. S.** (2004). Mastermind critically regulates Notch-mediated lymphoid cell fate decisions. *Blood* **104**, 1696–702.

**Maillard, I., Fang, T. and Pear, W. S.** (2005). Regulation of lymphoid development, differentiation, and function by the Notch pathway. *Annual review of immunology* **23**, 945–74.

**Manley, N. R. and Capecchi, M. R.** (1995). The role of *Hoxa-3* in mouse thymus and thyroid development. *Development (Cambridge, England)* **121**, 1989–2003.

**Masuda, K., Germeraad, W. T. V, Satoh, R., Itoi, M., Ikawa, T., Minato, N., Katsura, Y., Van Ewijk, W. and Kawamoto, H.** (2009). Notch activation in thymic epithelial cells induces development of thymic microenvironments. *Molecular immunology* **46**, 1756–67.

**Nehls, M., Kyewski, B., Messerle, M., Waldschutz, R., Schuddekopf, K., Smith, a. J. H. and Boehm, T.** (1996). Two Genetically Separable Steps in the Differentiation of Thymic Epithelium. *Science* **272**, 886–889.

**Neves, H., Weerkamp, F., Gomes, A. C., Naber, B. a E., Gameiro, P., Becker, J. D., Lúcio, P., Clode, N., Van Dongen, J. J. M., Staal, F. J. T., et al.** (2006). Effects of *Delta1* and *Jagged1* on early human hematopoiesis: correlation with expression of notch signaling-related genes in CD34+ cells. *Stem cells (Dayton, Ohio)* **24**, 1328–37.

**Neves, H., Dupin, E., Parreira, L. and Le Douarin, N. M.** (2012). Modulation of Bmp4 signalling in the epithelial-mesenchymal interactions that take place in early thymus and parathyroid development in avian embryos. *Developmental biology* **361**, 208–19.

**Nowell, C. S., Farley, A. M. and Blackburn, C. C.** (2007). Thymus organogenesis and development of the thymic stroma. *Methods in molecular biology (Clifton, N.J.)* **380**, 125–62.

**Okabe, M. and Graham, A.** (2004). The origin of the parathyroid gland. *Proceedings of the National Academy of Sciences of the United States of America* **101**, 17716–9.

**Owen, J. and Ritter, M.** (1969). Tissue interaction in the development of thymus lymphocytes. *The Journal of experimental medicine*.

**Palmer, E.** (2003). Negative selection--clearing out the bad apples from the T-cell repertoire. *Nature reviews. Immunology* **3**, 383–91.

**Parreira, L., Neves, H. and Simões, S.** (2003). Notch and lymphopoiesis: a view from the microenvironment. *Seminars in Immunology* **15**, 81–89.

**Patel, S. R., Gordon, J., Mahbub, F., Blackburn, C. C. and Manley, N. R.** (2006). Bmp4 and Noggin expression during early thymus and parathyroid organogenesis. *Gene expression patterns : GEP* **6**, 794–9.

**Peters, H., Neubuser, a., Kratochwil, K. and Balling, R.** (1998). *Pax9*-deficient mice lack pharyngeal pouch derivatives and teeth and exhibit craniofacial and limb abnormalities. *Genes & Development* **12**, 2735–2747.

**Pfaffl, M. W.** (2001). A new mathematical model for relative quantification in real-time RT-PCR. *Nucleic acids research* **29**, e45.

**Radtke, F., Fasnacht, N. and Macdonald, H. R.** (2010). Notch signaling in the immune system. *Immunity* **32**, 14–27.

**Rodewald, H.-R.** (2008). Thymus organogenesis. *Annual review of immunology* **26**, 355–88.

**Sato, Y., Kasai, T., Nakagawa, S., Tanabe, K., Watanabe, T., Kawakami, K. and Takahashi, Y.** (2007). Stable integration and conditional expression of electroporated transgenes in chicken embryos. *Developmental biology* **305**, 616–24.

**Seefeldt, B., Kasper, R., Seidel, T., Tinnefeld, P., Dietz, K.-J., Heilemann, M. and Sauer, M.** (2008). Fluorescent proteins for single-molecule fluorescence applications. *Journal of biophotonics* **1**, 74–82.

**Shanley, D. P., Aw, D., Manley, N. R. and Palmer, D. B.** (2009). An evolutionary perspective on the mechanisms of immunosenescence. *Trends in immunology* **30**, 374–81.

**Tarek, K., Mohamed, M., Omar, B. and Hassina, B.** (2012). Morpho-Histological Study of the Thymus of Broiler Chickens During Post-Hashing Age. *International Journal of Poultry Science* **11**, 78–80.

**Vilas-Boas, F., Fior, R., Swedlow, J. R., Storey, K. G. and Henrique, D.** (2011a). A novel reporter of notch signalling indicates regulated and random Notch activation during vertebrate neurogenesis. *BMC biology* **9**, 58.

**Wallin, J., Eibel, H., Neubüser, a, Wilting, J., Koseki, H. and Balling, R.** (1996). Pax1 is expressed during development of the thymus epithelium and is required for normal T-cell maturation. *Development (Cambridge, England)* **122**, 23–30.

**Watanabe, N., Tezuka, Y., Matsuno, K., Miyatani, S., Morimura, N., Yasuda, M., Fujimaki, R., Kuroda, K., Hiraki, Y., Hozumi, N., et al.** (2003). Suppression of differentiation and proliferation of early chondrogenic cells by Notch. *Journal of bone and mineral metabolism* **21**, 344–52.

**Watanabe, T., Saito, D., Tanabe, K., Suetsugu, R., Nakaya, Y., Nakagawa, S. and Takahashi, Y.** (2007). Tet-on inducible system combined with in ovo electroporation dissects multiple roles of genes in somitogenesis of chicken embryos. *Developmental biology* **305**, 625–36.

**Weinmaster, G.** (1997). The ins and outs of notch signaling. *Molecular and cellular neurosciences* **9**, 91–102.

**Xu, P.-X., Zheng, W., Laclef, C., Maire, P., Maas, R. L., Peters, H. and Xu, X.** (2002). Eya1 is required for the morphogenesis of mammalian thymus, parathyroid and thyroid. *Development (Cambridge, England)* **129**, 3033–44.

## 6. APPENDIX

**Table 6-1** Sequence of primers used in qRT-PCR assays and the respective product size and annealing temperature.

| Primer name | Forward primer (5'-3') | Reverse primer (5'-3') | Product size (bp) | Annealing temperature (°C) |
|---|---|---|---|---|
| **qGAPDH** | GAGTCCCCGCTCTTCACCACC | GGAAGAATTTGGAGGAGGAG | 97 | 62 |
| **cGAPDH** | GGTCATCCATGACAACTTTGG | CATCCACCGTCTTCTGTGTG | 83 | 62 |
| **Foxn1** | CGACATCGATGCTCTGAATC | AGGCTGTCATCCTTCAGCTC | 81 | 60 |
| **Gcm2** | TCAGAATTCCCAGAAAAAGAG | GAGGGCAGATTTTGCATGTT | 93 | 60 |
| **Hes5.1** | CCGACATCCTGGAGATGACT | AGGCATACCCTTCGCAGTAA | 99 | 60 |
| **DNMAML1** | CTGGAGCGCCAGCAAACCTT | TCATCAGTGCTTGCCGGCCC | 78 | 62 |
| **ICN1** | TAGTCAGCTGACGCGTGCTA | TTGCTCGACTCCGTCACTTTG | 106 | 60 |
| **GFP** | CGACAACCACTACCTGAGCA | GAACTCCAGCAGGACCATGT | 82 | 60 |

**Table 6-2** qRT-PCR primers for each evaluate gene and the respective sample used for calibration curves performing.

| Primer name | Gene | Sample used for calibration curve |
|---|---|---|
| **qGAPDH** | Quail GAPDH | Quail E9 thymus |
| **cGAPDH** | Chicken GAPDH | Chicken E18 thyroid |
| **Foxn1** | Foxn1 | Quail E9 thymus |
| **Gcm2** | Gcm2 | Quail E9 parathyroid |
| **Hes5.1** | Hes5.1 | Chicken Neural Tube 48h |
| **DNMAML1** | DNMAML1 constructs | pT2K-DNMAML1eGFP or pT2K-NLS-Cherry-DNMAML1eGFP |
| **ICN1** | ICN1 construct | pT2K-ICN1eGFP |
| **GFP** | GFP | OP9-vector |

**Table 6-3** *Foxn1* **(A)**, *Gcm2* **(B)** and *Hes5.1* **(C)** expression in the heterospecific association of tissues electroporated with the control vector (pT2K-BI-TREeGFP), pT2K-DNMAML1eGFP or pT2K-NLS-Cherry-DNMAML1eGFP.

**A**

| *Foxn1* | pT2K-BI-TREeGFP | DNMAML1 Low | DNMAML1 Medium | DNMAML1 High | NLS-DNMAML1 |
|---|---|---|---|---|---|
| Average | 1,000 | 0,132 | 0,411 | 0,504 | 0,446 |
| StDev | 1,129 | 0,100 | 0,420 | 0,567 | 0,406 |
| p-value | - | 0,314 | 0,469 | 0,546 | 0,493 |

**B**

| *Gcm2* | pT2K-BI-TREeGFP | DNMAML1 Low | DNMAML1 Medium | DNMAML1 High | NLS-DNMAML1 |
|---|---|---|---|---|---|
| Average | 1,000 | 0,427 | 3,251 | 5,983 | 1,036 |
| StDev | 1,330 | 0,414 | 2,510 | 4,069 | 1,002 |
| p-value | - | 0,540 | 0,262 | 0,159 | 0,972 |

**C**

| *Hes5.1* | pT2K-BI-TREeGFP | DNMAML1 Low | DNMAML1 Medium | DNMAML1 High | NLS-DNMAML1 |
|---|---|---|---|---|---|
| Average | 1,000 | 0,115 | 0,112 | 0,186 | 0,181 |
| StDev | 0,644 | 0,115 | 0,068 | 0,145 | 0,080 |
| p-value | - | 0,136 | 0,138 | 0,154 | 0,157 |

**Table 6-4** *Foxn1* **(A)**, *Gcm2* **(B)** and *Hes5.1* **(C)** expression in the heterospecific association of tissues electroporated with the control vector (pT2K-BI-TREeGFP) or pT2K-ICN1eGFP.

**A**

| *Foxn1* | pT2K-BI-TREeGFP | ICN1 Low/Medium | ICN1 High |
|---|---|---|---|
| Average | 1,000 | 0,133 | 0,229 |
| StDev | 1,129 | 0,061 | 0,085 |
| p-value | - | 0,315 | 0,358 |

**B**

| *Gcm2* | pT2K-BI-TREeGFP | ICN1 Low/Medium | ICN1 High |
|---|---|---|---|
| Average | 1,000 | 3,170 | 2,196 |
| StDev | 1,330 | 4,336 | 2,753 |
| p-value | - | 0,606 | 0,486 |

**C**

| *Hes5.1* | pT2K-BI-TREeGFP | ICN1 Low/Medium | ICN1 High |
|---|---|---|---|
| Average | 1,000 | 0,429 | 0,059 |
| StDev | 0,644 | 0,316 | 0,010 |
| p-value | - | 0,281 | 0,127 |

**Table 6-5 Buffers composition for multiple uses:** TAE 1X **(A)** and PBS 1x **(B)**.

**A**

| **TAE 1X** | |
|---|---|
| EDTA (pH 8) | 1mM |
| Acetic acid | 20mM |
| Tris base | 40mM |

**B**

| **PBS 1X** | |
|---|---|
| NaCl | 1mM |
| KCl | 20mM |
| $Na_2HO_4$ | 40mM |
| $KH_2PO_4$ | |
| Adjust pH to 7.4 with HCl | |

**Table 6-6 Bacterial growh media:** LB medium **(A)** and LB agar **(B)**

**A**

| **Lysogeny Broth (LB) medium** | |
|---|---|
| Tryptone | 1% |
| Yeast extract | 0.5% |
| NaCl | 1% |

**B**

| **LB agar** |
|---|
| 7.5g agar per 500mL of LB medium |